Canadian Technical Report of
Hydrography and Ocean Sciences 215

2001

Review of the Physical Oceanography of Sydney Harbour

by

B. Petrie
G. Bugden
T. Tedford
Y. Geshelin
C. Hannah

Ocean Sciences Division
Maritimes Region
Fisheries and Oceans Canada

Bedford Institute of Oceanography
P. O. Box 1006
Dartmouth, Nova Scotia
Canada B2Y 4A2

Cat. No. Fs 97-18/215 E ISSN: 0711-6764

Correct citation for this publication:

Petrie, B., G. Bugden, T. Tedford, Y. Geshelin and C. Hannah. 2001. Review of the Physical Oceanography of Sydney Harbour. Can. Tech. Rep. Hydrogr. Ocean Sci. 215: vii + 43 pp.

TABLE OF CONTENTS

LIST OF FIGURES

ABSTRACT

Petrie, B., G. Bugden, T. Tedford, Y. Geshelin and C. Hannah. 2001. Review of the Physical Oceanography of Sydney Harbour. Can. Tech. Rep. Hydrogr. Ocean Sci. 215: vii + 43 pp.

Two studies of the physical oceanography of Sydney Harbour were conducted one in 1987-88 and the second in 1992-93. They included moored current meters and hydrographic surveys of the harbour. Our analysis of these data has found that: the distributions of temperature and salinity are generally what would be expected for an estuary forced by weak freshwater discharge; mean flows are consistent with an estuarine circulation pattern, i.e., outflow near the surface and inflow near the bottom; an individual current observation is generally less than 10 cm s^{-1}; high frequency seiches that depend on the dimensions of the harbour can contribute significantly to the flow with current amplitudes that can be up to 10 times greater than the largest tidal component; low frequency flows associated with storms can lead to the strongest currents seen in the harbour; and, sediment transport modelling of the strongest event seen in the current records led to a net displacement of sediment towards the head of the harbour.

RÉSUMÉ

Petrie, B., G. Bugden, T. Tedford, Y. Geshelin and C. Hannah. 2001. Review of the Physical Oceanography of Sydney Harbour. Can. Tech. Rep. Hydrogr. Ocean Sci. 215: vii + 43 pp.

Deux études d'océanographie physique ont été réalisées dans le port de Sydney, l'une en 1987-1988 et l'autre en 1992-1993. Elles comportaient des mesures par courantomètres mouillés et des levés hydrographiques du port. Notre analyse des données recueillies à ces occasions a révélé que les distributions de la température et de la salinité sont en général conformes à ce qu'on peut attendre d'un estuaire assujetti à un faible écoulement d'eau douce; les débits moyens correspondent à un régime de circulation estuarienne, c'est-à-dire à un débit sortant près de la surface et à un débit entrant près du fond; l'observation d'un courant révèle un débit généralement inférieur à 10 cm s^{-1}; des seiches de haute fréquence, liées aux dimensions du port, peuvent contribuer considérablement au débit et produire des amplitudes de courant qui sont jusqu'à 10 fois plus grandes que les plus fortes composantes de la marée; les flux de basse fréquence découlant des tempêtes peuvent être à l'origine des plus forts courants observés dans le port et la modélisation du transport de sédiments associé aux plus grands phénomènes enregistrés à ce jour aboutissait à un déplacement net des sédiments vers le fond du port.

1. Introduction

Sydney Harbour, situated in eastern Cape Breton, Nova Scotia, opens onto Sydney Bight, the area of ocean bordered by Cabot Strait, Laurentian Channel and the eastern Scotian Shelf. The harbour is 'Y' shaped with the seaward arm dividing into a northwest and south arm (Fig. 1). The south arm is about 10 km long, 1 km wide and 10 m deep. Sydney River empties into the harbour at its head and has a peak monthly inflow of about 21 $m^3 s^{-1}$ in April and a minimum inflow of about 5 $m^3 s^{-1}$ in July and August (Gregory et al. 1993). The south arm of the harbour will be the main focus of this report.

A number of physical oceanographic studies have been carried out in Sydney Harbour over the past century. Easton (1972) reports a study by Honda and Dawson (1911) who found sea level oscillations with amplitudes of 0.15 m and periods of 2 h recorded by a tide gauge in North Sydney. Honda and Dawson (1911) assumed that the oscillations were generated independently in each arm of the harbour. They estimated fundamental periods of 2 and 2.2 h, in good agreement with the observations.

Easton (1972) refined the calculations of Honda and Dawson (1911) by constructing an analytical solution for a three channel model of the harbour with seaward, south and northwest arms. For mean water level, he found resonant periods of 103, 52, 36.6 and 22.5 minutes for the first four modes of the harbour as a whole. The first modes for the individual channels had periods of 31 (seaward), 58 (south) and 42 (northwest) minutes. Easton also solved the finite difference forms of the governing equations, obtaining resonant periods of 107, 39, 31.5 and 24 minutes for the harbour as a whole, different than the analytical solutions. A correction for the basin opening onto the ocean increased the period of the first mode from 107 to 124 minutes. Easton analyzed 1970 sea level records from North Sydney and found distinct oscillations with periods of 120 to 130 minutes. Amplitudes as high as 0.3 m were observed. He concluded that the seiches were initiated by storms and were probably the response of the harbour to external edge waves, whose periods he estimated as about 152 minutes.

A number of environmental studies that include physical oceanographic components have been conducted in Sydney Harbour including Lane (1988) and ASA (1994). The Lane (1988) study included hydrographic surveys in August and November of 1987 and in January of 1988, drogue tracking for about 8 hours in August and November (ice prevented drogue releases in January), and 2 current meter moorings. One mooring (46^o 11.38'; 60^o 12.96' at 13 m, about 1 m off the bottom) was located outside of the south arm of the harbour and ran from August 24 to November 9, 1987. A second moored current meter in the south arm ran from January 12, 1988 to April 27, 1988 (46^o 11.31'; 60^o 12.92' at 14.6 m, about 1 m off the bottom).

The ASA study consisted of hydrographic sections along the harbour, acoustic Doppler current profiles from a ship-mounted instrument (ADCP) along and across the inlet, and moored current meters in the harbour. The moored current meter data were from a single Aanderaa instrument deployed at about 10.8 m depth and located off Muggah

Creek from August 4 to September 2, 1992. A bottom mounted ADCP was deployed in roughly the same site from July 25-August 24, 1993. The locations of these instruments and the current meter from the Lane study are shown in Fig. 2.

In October 2000, four instrument packages were moored in Sydney Harbour by the Ocean Sciences Division (OSD) of Fisheries and Oceans as part of an overall study (see Fig. 2). Two ADCP moorings are located off Muggah Creek while 2 moorings consisting of near-surface and near-bottom temperature-conductivity recorders are sited along the harbour on either side of the ADCP moorings. These instruments were recovered in May of 2001. Analyses of the results from this observation program will be completed in 2001-02. In the meantime, in order to learn as much as we can about the circulation in the harbour, we have to examined the archived data from the Lane and ASA studies.

2. Lane Study 1987-1988

Lane (1988) presents 3 hydrographic sections from August and November of 1987 and January of 1988 (redrawn in Fig. 3). The August section shows temperature differences of about 5^{o}C from the surface (19^{o}C) to the bottom (14^{o}C). Salinity did not show a strong influence of freshwater inflow, with a difference of about 1 from surface to bottom. On the other hand the salinity was somewhat less than the average surface value of 29.2 in Sydney Bight at this time of year (Petrie et al. 1996). Thus some nearshore influence of freshwater inflow was present. In November the temperature variation in the harbour was small, amounting to about 1^{o}C; in contrast, there was strong evidence of the influence of river input to the inlet. Near the head of the harbour, salinity reached 18, whereas towards the mouth it was between 26 and 27. The highest salinities of 28 were recorded near bottom at the head of the inlet. In Sydney Bight at this time the typical 0-10 m salinity is about 30. The January section was limited in extent because of the presence of ice in the harbour. Only the outer half of the inlet was sampled. Temperature showed little variation over the entire depth; salinity increased from 25.5 in mid-harbour to 27 at the mouth. A typical salinity in Sydney Bight would be about 30.5 at this time of year.

Overall, the hydrographic data indicate that Sydney Harbour is generally, and sometimes strongly, influenced by freshwater inflow, and that strong thermal stratification can develop at least during the summer months.

The current meter from 1987 was located in the seaward arm of the harbour off South Bar (Fig. 1, 4) at 13 m, about 1 m above the bottom. Lane reports a mean flow of 2.4 cm s^{-1} at 216^{o}, i.e. basically across the mouth of the south arm of the harbour. The major tidal current was the M_2 constituent at 6.9 cm s^{-1} in the north-south direction. Lane did not report on the results of the current meter that was located inside the mouth of the south arm (Fig. 2). We present an analysis of this record below.

The mean current from the January-April, 14.6 m current meter was 1.35 cm s^{-1} along 162^{o}, i.e., along the local axis and into the harbour (Fig. 4). The direction of this current is what one would expect if the circulation in south arm of the harbour were estuarine. In a simple estuary, fresh water inflow at the head of the inlet would force a near surface outflow. The outflow would entrain subsurface water and would increase its salinity. Subsurface water would flow into the harbour to compensate for the entrained water. This gives rise to the two layer circulation that is often observed in coastal inlets where there is significant fresh water inflow.

The time series of current speed, direction, along- and across-harbour current show that the flow is highly variable with maximum speeds of nearly 30 cm s^{-1} (Fig. 5). The tendency for the current direction to align roughly along 180^{o} indicates that the circulation is dominated by along-harbour flow. This is further strengthened by the plots of the along-harbour component of flow (positive along 160.5^{o}). It is evident from this plot that the estuarine sense of the flow is subject to considerable variability. While the mean flow may indeed be into the harbour, there are numerous occasions when the current is out of the harbour. It is also apparent that the along-harbour current is considerably larger than the across- harbour component (positive towards 70.5^{o}).

The progressive vector plot of the current shows the path that a water particle would take if it experienced the flow measured by the current meter (Fig. 6). This indicates that inflow dominates, in spite of the along-harbour variability shown in Fig. 5. Given that the inlet is roughly 10 km long, during the roughly 4 months the instrument was in place, the current would carry a parcel of water about 120 km towards the head of the inlet, that is, roughly 12 times the harbour length. Of course, water from the lower layer is entrained by the assumed, near surface, outgoing flow. However, this could mean that near-bottom particulate material would tend to be transported and potentially deposited from the area off Muggah Creek towards Sydney River. We shall examine the distribution of some bottom sediment surveys later to see if this is so. The progressive vector diagram also indicates that the inward transport occurred mainly because of three events: one near the beginning of the record (about January 16), one near the middle (February 29), and one towards the end (April 17). This is demonstrated by the spacing between day markers in the plot, where a large space between dots indicates a large movement on those particular days. These events are also seen in the time series plots of direction and along-harbour flow (Fig. 5) as periods when the direction was steady along roughly 160^{o} and consequently the along-harbour flow remained positive. We shall examine these events more closely to try to determine their causes.

The histograms of current speed and direction indicate that for the most part the current is below 0.1 m s^{-1} . Moreover the direction is predominantly into or out of the harbour, with the former being the favoured mode for the current.

The current spectrum

The power spectrum of a data series is the distribution of variance of the record as a function of frequency. The spectrum of the 1988 current meter time series has three

notable features (Fig. 7), namely, it is red, that is, the power increases as frequency decreases. This indicates that most of the variance is accounted for by low frequency (long period) oscillations in the harbour. Secondly, in the low frequency part of the spectrum there is a distinct peak at roughly 2 cpd that corresponds to the semi-diurnal tidal band. A harmonic analysis in this band (in fact for a period of 12.42 hours, corresponding to the principal lunar constituent M_2) indicates a tidal flow with an amplitude 0.017 m s^{-1} . The integral of the variance from periods of 11 to 13h gives a standard deviation of 0.016 m s^{-1}. Thirdly, there is a broad band of enhanced variance between 9 and 13 cpd (periods of 2.7 and 1.8 hours) that, on average, corresponds to a current of 0.016 m s^{-1}, that is about the same magnitude as the semi-diurnal tides. This band occurs at or near the seiche periods that were observed by Honda and Dawson (1911) and Easton (1972).

To examine the seiche components more closely, we filtered the original time series to create a high pass version, i.e. the low frequency energy was removed (Fig. 8). This series shows that while the average seiche current amplitude is 0.016 m s^{-1}, the instantaneous amplitude had a maximum value of 0.13 m s^{-1}, and in these cases makes a larger contribution to the flow than does the strongest tidal component.

Temperature

The temperature time series features part of the strong annual cycle of temperature from the start of the record until the finish (Fig. 9). Temperature at the beginning of the record already showed the effects of winter cooling with values ranging from about -0.5 to -1.5^{o}C. A broad temperature minimum was reached from about mid-February to early April. With the onset of spring warming, temperature began to increase in early April, continuing until the end of the record. We expect the warming trend to occur first in the surface layer because of its contact with the atmosphere. Mixing processes would eventually cause the temperature to increase in the lower layers.

One of the outstanding features of this record is the transient warming event that occurred between April 12-16. This event featured elevated temperatures for approximately 5 days composed of overall warming and semi-diurnal oscillations. We think that this event was not primarily one in which mixing occurred from the surface, but rather a displacement of sub-surface waters and subsequent restoration of these waters as the forces responsible for the event subsided. We shall examine this event in more detail later.

Sea level

The observations from North Sydney during the current meter deployment demonstrate the tidal nature of the sea level variability (Fig. 10). The largest component, M_2, has an amplitude of 0.37 m; the components N_2, S_2, K_1, and O_1 have amplitudes of 0.08, 0.11, 0.08 and 0.08 m. The spring-neap cycle, beating at about 15 d, is also evident in the record. A 25 h running mean filter was applied to the hourly dataset and the result shows that there was considerable low frequency variability (Fig. 10). Peak-to-peak amplitudes of nearly 0.7 m are evident. The adjusted sea level record, which has the effect of changing atmospheric pressure removed, shows similar but reduced variability.

It should be noted that the sea level gauge at North Sydney is located in the main arm of the harbour, across from the mouth of the south arm.

Wind, a primary forcing mechanism

During the mooring period, wind speed recorded at Sydney Airport was generally between 5 and 10 m s^{-1} (Fig. 11). Directions varied throughout the record but featured periods when the wind blew steadily in a narrow band. The most striking example occurs in early April when the wind maintained a relatively steady speed of 5-10 m s^{-1} and a direction that slowly changed from about 270 to 180^{o}. Wind stress varied between 0 and 0.33 Pa. The wind measured at Sable Island would be more representative of conditions over the open ocean. Wind speed, stress and direction recorded at Sable resembled the Sydney Airport observations but with higher speeds, 10–15 m s^{-1}, and stresses, 0.25-0.5 Pa. The bottom temperature response that accompanied this forcing is interesting. Throughout most of the event there was no ocean temperature response measured by the instrument. However, near the end of the event the temperature increased abruptly by nearly a degree. There were some rapid oscillations of temperature until it resumed its seasonal increase (refer also to Fig. 9).

Freshwater runoff

Daily mean freshwater inflow from nearby Salmon River and the ratio of drainage basin area (269 km^2 /199 km^2) were used to create a time series of inflow into the south arm of Sydney Harbour for the mooring period (Fig. 12). There were a number of episodes of high runoff with the largest at 126 m^3 s^{-1} occurring on April 11. This peak overlapped the persistent wind event mentioned above.

The April wind-freshwater inflow event

This event is notable because of the nature of the wind forcing, the slowly changing direction and relatively high stress, and the freshwater inflow, a broad four day peak with a maximum daily rate of 126 m^3 s^{-1}. In the harbour, the temperature response consisted of an abrupt increase that occurred several days after the forcing began; the current showed high variability during the period when wind stress and inflow were high, with the strongest current inflow occurring when the winds and freshwater flow abated. The current flowing into the harbour was sustained for about three days (Fig. 5, 11,12).

The details of the event are shown in Fig. 13 and 14. Wind and wind stress increased towards the west on April 5 (note that the oceanographic convention for direction, i.e. direction to, is used for the wind data). The wind remained in this direction for nearly 4 days. Then wind direction slowly rotated such that by the 12th it was towards the south. It remained towards the south until about midday on the 15th. Wind speed and stress started to decrease on the 12th of April, essentially vanishing by the 16th. The freshwater inflow had a background level of about 25 m^3 s^{-1} that began increasing about the 9th and reached its peak value of 126 m^3 s^{-1} on the 11th. By the 13th it had fallen to the background level. The current response consisted of essentially zero net flow from April 6-16, followed by a net inflow that reached a peak of about 0.24 m s^{-1} over the next three days. Temperature showed an abrupt increase on the 12th of April, following peak

inflow and stress. Considerable variability occurred over the next 5 days. The variations were primarily at the semi-diurnal period. Adjusted sea level reached a maximum value of 12.9 cm above the April mean on the 11th, i.e., near the peak freshwater inflow and peak stress.

The wind stress, which generally had a component along the harbour from the mouth to the head, would act to set up sea level. This pressure gradient would drive the deeper waters out of the harbour, and caused the surface layer to thicken until the pressure along the bottom approached zero and a dynamical balance between the stress and pressure gradient was established. There were no temperature measurements from the surface layer taken at this time. However, the mean climatological surface temperatures outside the harbour in Sydney Bight should be about -0.5^{0}C (Petrie et al. 1996). The thickening surface layer would move down the harbour, eventually intersecting the instrument and raise the temperature it recorded. Tidal movements could carry this internal front back and forth across the instrument causing oscillations in temperature. When the forcing disappeared, cooler bottom waters would rush back into the harbour and seasonal warming would resume.

Freshwater inflow, which occurs mostly at the head of the harbour at Sydney River, would also tend to raise sea level. However, its effect on currents would oppose the action of the wind. The freshwater inflow would tend to drive a surface current out of the harbour, leading to a return flow at depth. So there are 2 competing mechanisms to examine.

Setup caused by wind

In steady state with the wind stress (τ) along the harbour towards the head, the current or at least its integral over depth would be zero. Taking the water density as constant (i.e., not allowing for along harbour density variations) then there would be a balance between sea surface slope ($\partial\zeta/\partial y$) and wind stress:

$$g\partial\zeta/\partial y = (1/\rho_o)\partial\tau/\partial z$$

Assuming that τ drops to zero over a depth h_o, the sea surface slope is

$$\partial\zeta/\partial y = (1/g\rho_o)\tau/h_o$$

In the event described above, τ has a peak value of about 0.3 Pa. Then, if we take h_o initially as half the depth, $\approx$5 m, ∂y=10 km and ρ_o=1025 kg m^{-3},

$$\Delta\zeta = \partial\zeta = 6\,\mathrm{cm}$$

This is about half of the maximum setup of 12.9 cm relative to the April mean occurred on the 11th. Note also that the sea level gauge is opposite the mouth of the south arm of the harbour. The setup at the head could be different than that measured at the North

Sydney gauge. The lower layer, i.e., deeper than 5 m, would feel an unbalanced pressure gradient. This would drive the bottom waters out of the harbour. The time, t, to empty the harbour would be roughly

$$h_o vt = Lh'$$

where v is the current speed, L is the length of the harbour and h' is the lower layer depth.

Taking $h_o v$ initially as

$$h_o v = (\tau / \rho_o)t$$

we have

$$t^2 = (\rho_o Lh'/\tau)$$

giving t = 3.6 h. This time represents a first estimate of the time required for internal adjustment of the pycnocline, the density interface between the upper and lower layer, to adjust to the surface pressure gradient. This is a lower bound for several reasons. First the surface setup would require an internal adjustment or setdown of approximately $(\rho_o/\Delta\rho)\Delta\varsigma$; this is of order (1025/0.5)*6 cm or about 120 m. Thus the entire harbour would have to empty. Secondly, as the surface layer deepened, the depth h_o of the upper layer would increase causing a readjustment, in fact a decrease, of the pressure gradient. This would decrease the bottom layer velocity and consequently increase the adjustment time. Third, the approximation for the velocity gives a very large value of the bottom flow of nearly 1 m s^{-1}. Before such a speed could be attained, bottom friction would be important and limit the velocity.

Consider the following balance for the lower layer:

$$\partial v / \partial t = -g\partial\varsigma / \partial y - c_d v|v| / h'$$

where c_d is the drag coefficient and the last term represents bottom friction. Over the course of the adjustment, the depth of the upper layer will increase from its original value to the total depth since the indication is that the entire harbour is emptied. To simplify the problem we shall take the surface gradient as given by $(1/2)\{\tau/(g\rho_o h_o) + \tau/(g\rho_o h_T)\}$, where h_T is the total depth. This is substituted into the non-linear equation and the problem solved numerically for a wind stress that changes from 0 to 0.3 Pa in 4 days similar to the observations at Sydney Airport. Under these conditions, the time scale increases to 1.65 days for all of the water to be replaced in the harbour. The maximum outflow velocity would be 15 cm s^{-1}, a value that exceeds the observed velocities that in effect oscillate about 0 from April 4 to 16 (Fig. 13). On the other hand, if we take the low frequency, along-harbour wind stress (Fig. 14) that reached a maximum value of about 0.2 Pa after 3 days, we also get a maximum current of about

15 cm s^{-1} but a replacement time of 2.8 days. This is approximately when the temperature increased (Fig. 14). We do not have hydrographic data from the harbour at or even close to the event, therefore, we do not know some of the basic parameters, such as layer depths, in situ temperatures etc., that we have used in these calculations. However, under particular, and not unreasonable, circumstances, we can find a time scale for internal mass adjustment in the harbour that fits with the time scale of temperature change recorded by the near bottom current meter.

After the peak in the low-pass wind stress on April 12th , the stress slowly decreases to about 0.1 Pa over 3 days. This could maintain the warmer water at the current meter site. On the other hand, sea level decreased to the April mean value by the 15th of April, i.e., the setup appears to have ceased. Note though that the gauge was opposite the mouth of the south arm of the harbour not at the head which would have provided a more definitive record for following the changes of sea level. On the 15th, wind stress drops to zero (Fig. 14). It took 1.5 days for water temperatures to return to the values before the event. This implies that a large area outside of the south arm must have been flushed. Strong inflowing currents coincide with the reappearance of the cold near-bottom waters that were present before the event. If the front associated with the cold water return moved at a characteristic speed of 15 cm s^{-1} (Fig. 14), then the front could have been located roughly 20 km from the mouth of the south arm. It is about 10 km to the mouth of Sydney Harbour proper from the south arm.

Response to freshwater inflow

Hansen and Rattray (1965) considered the buoyancy driven flow in estuaries and derived restricted solutions for the gravitational circulation complemented by wind stress. With no wind stress, the circulation is driven by the along inlet density gradient and is generally accompanied by vertical stratification. The state of the inlet is often described by the intensity of the gravitational circulation u/u_{fw}, where u is the mean current at the surface and u_{fw} is the freshwater discharge velocity, and by the strength of the vertical stratification $\Delta S/S$, where ΔS is the difference in salinity between the bottom and the surface, and S is the depth averaged salinity. For Sydney Harbour, these variables are listed in the table below.

Month	$\Delta S/S$	Runoff(m^3 s^{-1})	u(m s^{-1})	u_{fw} (m s^{-1})
Jan.	0.05	12.1		0.0012
Aug.	0.02	4.9	0.065	0.0005
Nov.	0.12	16.9		0.0017

Hansen and Rattray (1966) derived a classification scheme based on the parameters $\Delta S/S$ and u/u_{fw}. For $\Delta S/S=0.02$ and $u/u_{fw}=130$, Sydney Harbour in August is a type 2a estuary that should exhibit flow reversals with depth and with major roles played by the down-estuary advective salt flux and the up-estuary diffusive salt flux. The salinity stratification should be weak. Another important parameter in the Hanson-Rattray model is νRa, where ν is a constant that depends on the dimensionless wind stress T, a tidal mixing parameter M, and Ra, the “estuarine Raleigh number”. For T=0, the flow is bi-directional for $\nu Ra>30$.

We have constructed the depth dependent velocity profiles for three cases of freshwater runoff: 25, 75, and 125 $m^3 s^{-1}$ representing the range of freshwater inflow during the current event of April 1988 (Fig. 15). The solutions show a weak outflow in the surface layer with a maximum value of about 0.02 m s^{-1} for a freshwater inflow of 125 $m^3 s^{-1}$. The return flow is particularly weak and should not affect the adjustment time scales appreciably. For freshwater inflow of 25, 75 and 125 $m^3 s^{-1}$, νRa is equal to 51, 33 and 23. The model predicts no return flow for the case with T=0, νRa =23 (Fig. 15). It is important to remember that the Hansen-Rattray model represents a restricted set of solutions. We are using the model to give an estimate of the strength of the buoyancy driven flow.

3. ASA current meter and hydrographic surveys of Sydney Harbour, 1992 and 1993

In August 1992, ASA (1994) deployed a single current meter at 10.8 m in a total water depth of about 16 m off Muggah Creek (Fig. 2) and conducted hydrographic surveys using an RS5 temperature and salinity probe and a SeaBird CTD. Current speeds were extremely weak with maximums of about 0.15 m s^{-1}; speeds were generally less than 0.05 m s^{-1} (Fig. 16). The mean current was 0.0028 m s^{-1} at 342^o, that is in a direction generally out of the harbour. This mean flow is not inconsistent with the expectations from the Hansen-Rattray solutions (Fig. 15), weak outflows most of the water depth with an even weaker inflow at the bottom. Temperature increased from about 13^{o}C at the beginning of the record to 18^{o}C at the end. Salinity fell from 29.5 to 28.7 ASA (1994) shows RS5 and SeaBird data collected from August 12 to 20 and December 16. Figure 17 shows CTD stations collected in the south arm of the harbour on August 20. The data indicate shallower temperatures and salinities increasing towards the mouth of the arm, the salinity variation in keeping with estuarine circulation. The deeper salinities do not vary as expected for a simple estuary because the salinities at the station closest to the mouth of the arm are the lowest. December profiles had stronger near surface salinity gradients (Fig. 18). Shallow salinities showed an estuarine pattern with salinity increasing by about 2 from near the head of the arm to the mouth. Deeper salinities showed a similar variation but with a considerably reduced gradient. Deep temperatures were higher near the mouth of the harbour and decreased towards the head. Near-surface temperatures, with the exception of the station nearest the head, behaved similarly. The thermoclines and haloclines varied from 2-7 m depth.

In July-August 1993, ASA (1994) deployed a bottom mounted Acoustic Doppler Current Profiler (ADCP) off Muggah Creek (Fig. 2). This instrument provided estimates of the velocity at 1 m intervals to within about 2 m of the surface depending on the state of the tide. The upper 2 bins (nominally 2 and 3 m) occasionally had missing points in all likelihood caused by lowered sea level and consequently interference from the strong surface reflection. The mean currents from this record are displayed on Fig. 4 for selected depths and Fig. 19 for the complete profile. For the greater part of the water column, the current is generally towards the head of the harbour. At 3 m and more so

at 2 m, the current reverses and is directed towards the mouth in an estuarine-like circulation. Current speed is weak, about 0.5 to 2 cm s^{-1}, at all depths below 2 m, where the flow is about 6 cm s^{-1}.

The current speeds were generally low at all depth levels. Combining all levels from 2 to 15 m, about 94% of the observations had speeds less than 10 cm s^{-1}, only 1% were greater than 20 cm s^{-1}, and only 1 data value was between 36 and 38 cm s^{-1}, the last bin in the 2 cm s^{-1} resolution histogram. The deepest bin, crucial for the resuspension of sediment, had 98% of its speeds less than 10 cm s^{-1}, and a maximum value of 15.4 cm s^{-1}. In general, currents were dominated by along-harbour flows. The current variations in the along- harbour direction (taken as 337^{o} for all depths) are shown in Fig. 20 for selected depth levels. Note that these currents are about 2.5 times larger than the flows shown in the ASA (1994) report. We suspect that that an error occurred in the earlier processing that led to this difference. This conclusion was reached after consultation with ASA; as in many cases examining archived data and because of the potential uncertainties in their processing, it represents the most likely conclusion that we can make now. The low frequency fluctuations in these records give an indication that estuarine-like circulation occurs for the variable as well as for the “mean” flows. For example, near the beginning of the record, the current at 3 m is predominantly out of the harbour, whereas the deeper flow, particularly at 10 m is in the opposite direction. This is also true of the higher frequency events that take place about August 9 and 15. In these cases the shallow current is into the harbour and the deeper flow out in a reverse estuarine mode. The last week or so of the records show a slow fluctuation from outflow to inflow at the 3 m level, accompanied by the opposite variation at depth, most notable a 10 m.

Daily mean currents clearly demonstrate the current reversals that occur over the water column (Fig. 21). Periods of estuarine and reverse estuarine flow are evident with the former the most dominant mode of circulation.

4. Sediment movement

We have used the bblt (bottom boundary layer transport) model driven by in situ current observations (Hannah et al. 1995; Tedford et al. 2001) to examine the resuspension and movement of sediment in Sydney Harbour. The bblt model of suspended sediment transport works in the following way. There is an initial distribution of sediment on the bottom and in the water column. In our simulations all of the sediment is on the bottom initially. The currents and the bottom stress increase until a critical value of the stress is reached; at that point all of the sediment becomes suspended. The suspended sediment is sheared by the vertical structure of the horizontal currents; the suspended sediment is also smeared by the vertical mixing. Finally, the currents weaken and the sediment settles back to the bottom with a broader distribution and a new centre of mass.

The original formulation of the model had a single critical stress at which all of the particles would be suspended. However, in an environment like Sydney Harbour where depths vary significantly, and the shoreline and bottom features can provide sheltered areas, we expect that a single critical stress will not accurately describe the potential to suspend bottom sediment. Milligan and co-workers have collected a series of bottom grabs throughout the harbour and estimated critical bottom stresses from size distributions of particles (T. Milligan, Marine Environmental Sciences Division, Bedford Institute of Oceanography, personal communication, Fig. 22). The magnitudes of their critical bottom stress estimates are broadly distributed and indicate that a single value would be a very crude approximation to use for the harbour. Consequently, the resuspension module of the model was modified to allow the partition of the sediment between a suspended fraction that moved with the currents and fraction that stayed in place on the bottom. As bottom stress increases, a larger fraction of the bottom sediments would be suspended. The function describing the dependence of the ratio of the suspended fraction to the total sediment on the friction velocity, u_*, was determined from 18 estimates of critical stress made by Milligan and co-workers from approximately $\pm$1 km along the harbour from the mouth of Muggah Creek, a likely source of contaminated sediment (Fig. 23). For example, at low friction velocities, little of the sediment in the model is suspended; at a friction velocity of about 0.008 m s^{-1} about 10% of the bottom sediment is suspended; as bottom stress increases the amount of suspended sediment increases rapidly so that at a friction velocity of about 0.015 m s^{-1} about 90% of the bottom sediment is suspended. The friction velocity, u_*, is determined in the model from the bottom stress, τ_b, as $\{|\tau_b|/\rho_0\}^{1/2} = \{C_d|u_b|^2\}^{1/2}$, where ρ_0 is the water density, C_d is the drag coefficient and u_b is the velocity at the bottom level of the model. The bottom of the model is assumed to be in a constant stress layer.

The model requires a current profile over the entire water depth to determine the dispersion and transport of suspended material. We constructed an estuarine-like, along-harbour velocity profile from the 1988 near-bottom current meter record (Section 2) in the following manner. Based on other current meter results (ADCP observations) and some CTD data that were not contemporaneous with the 1988 mooring, we divided the water column into an upper layer depth of 4 m, and a lower layer that extended from 4 m to the bottom. The observed along-harbour current was assumed to contain barotropic (depth-independent) and baroclinic (depth-dependent) components. We assumed that the high frequency flows caused by tides and seiches were predominantly barotropic and that the lower frequency flows were baroclinic. We separated the current components using Fourier decomposition and recombined them in the upper and lower layers to create a velocity profile. The lower layer current was the flow measured by the instrument. The upper layer flow consisted of the barotropic, high frequency components derived from the current meter record combined with the baroclinic, lower frequency components (also derived from the Fourier decomposition of the current meter record) but with their phases changed by 180^o. Thus the baroclinic components in the upper layer are in the opposite direction to those in the lower layer. The baroclinic flow was assumed non-divergent for this simulation, i.e.,

$V_{0\text{-}4m}$*(Cross-sectional Area)$_{0\text{-}4m}$ = $V_{4m\text{-}btm}$*(Cross-sectional Area)$_{4m\text{-}btm}$.

The weaker across-harbour component was taken as the same at all depths. Our formulation of the depth varying component neglects the net flow out of the harbour that is equal to the freshwater inflow. For the event discussed below, this would lead to a maximum error of about 0.0125 m s^{-1} (=125 m^3 s^{-1}/(4 m * 1000 m), i.e. the peak freshwater outflow (Fig. 12), divided by the upper layer depth and the harbour width). This compares to a maximum current during the event of about 0.25 m s^{-1}. Another potential error comes from low frequency changes of sea level within the harbour. From Fig. 13, we estimate that a maximum change of about 0.1 m can occur over 2.5 days giving rise to an error of about 0.0002 m s^{-1} (0.1*800*5000/(2.5*86400*10*1000), i.e. the sea level displacement times the average width and the length of the harbour landward of Muggah Creek, divided by the time, the depth and the width of the harbour off Muggah Creek). These errors are relatively small and probably less crucial than other model assumptions.

The currents are assumed not to vary with horizontal distance throughout the modelled region, i.e. the model does not know that the harbour has an end, varies its cross-section or opens onto the ocean. The implication for its application to Sydney Harbour using the 1988 data would be that the sediment transport would be overestimated. The two major factors for this conclusion are: the finite length of the harbour means that at the head the only flow would be from the river; using data from within the harbour would overestimate flow strength. Secondly, the observations are from farther out the harbour than Muggah Creek, again making it likely that they are stronger than would be experienced off the Creek. On the other hand, the cross section of the harbour decreases in the vicinity of the Creek which would tend to produce higher current speeds.

The 1993 ADCP data (Section 3) provided a complete velocity profile that could be used directly by the bblt model.

The model was run for both datasets to determine the time variation of the fraction of suspended material in the water column. In all of our simulations we started with 100,000 particles so that a suspended fraction of 0.6 means that 60,000 particles are in the water column, 40,000 on the bottom. The time series of suspended fraction for the 1988 and 1993 periods when the current meters were in place are shown in Fig. 24. There is a dramatic contrast between the time series covering the 2 mooring periods. The July-August 1993 mooring featured weak current velocities and consequently few instances when substantial amounts of sediment particles were suspended within the model. The January-April 1988 current record featured larger velocities leading to more suspended particles, more often. The strongest events occurred in February and April (Fig. 25). Complete simulations were made only for this last event which was the longer of the two.

The details of the April event are shown in Fig. 26. Each panel is separated by 12 h over a four day period from April 17-21. The vertical axis is the height above the bottom; the horizontal axis is the distance from Muggah Creek at 0, with negative

(positive) distance toward the head (mouth) of the harbour. The percentage of particles suspended is next to each panel; e.g. in the first panel 0.8% or 800 particles of the 100,000 are suspended. The colourbar is a percentage scale tailored to each panel; e.g. near the origin in the first panel, the red pixel indicates that roughly 20% of the particles that are suspended are in this pixel. The first instance when the majority of particles, 96.2%, are suspended is seen in the panel for April 19, 1:12. The currents are moving the deep particles towards the head of the harbour, while the particles near the surface are moving towards the mouth. Note that the particles near the surface would first have to move through parts of the water column that were moving towards the head. This is why their net integrated displacement at this time is towards the head. The model run indicates some relaxation over the next 12 h, followed by another major resuspension. The last 2 panels show a gradual decay of the event with a net movement of particles towards the head of the harbour. The final result indicates that particles in general would have been transported towards the head of the harbour with the bulk potentially carried 5-10 km.

Vandermeulen (1989) presented the results of surveys for PAH and heavy metal sampling in Sydney Harbour. His redrawn plot for PAH bottom contamination of the harbour indicates that the higher values are generally found towards the head of the harbour (Fig. 27). Moreover, the concentrations fall less rapidly towards the head (an e-folding scale of 1 km than they do towards the mouth (an e-folding scale of 0.43 km). Similar results are shown by Ernst et al. (1999) for a 1995 survey of PAH in the harbour. This is consistent with the strong event and with the overall statistics from the 1988 winter current meter record (Section 2) and the bottom ADCP summer current record from 1993 (Section 3). The 1988 record had flow into (out of) the harbour for 58% (42%) of the time with current of 0.049 m s^{-1} (0.035 m s^{-1}); the 1993 record had flow into (out of) the harbour for 57% (43%) of the time with current of 0.033 m s^{-1} (0.030 m s^{-1}). Thus for both winter and summer, the flow is into the harbour for a greater percentage of the time and has a higher speed.

5. Summary

Our examination of existing data from Sydney Harbour has been useful and has led to the following conclusions:

- the distribution of salinity is generally consistent with what would be expected for an estuary with a significant fresh water forced component of the circulation; some of the hydrographic data do not fit this pattern indicating other processes at work. The overall role of the fresh water inflow could be better determined with in situ temperature-salinity recorders and contemporaneous current meters. This could overcome the aliasing that can occur from infrequent hydrographic surveys.

- mean flows derived from in situ current meters are consistent with an estuarine-like circulation pattern, outflow at near-surface depths, inflow deeper and at the bottom;

- current speeds in the harbour are weak in summer and winter; at most times currents are less than 10 cm s^{-1};

- high frequency currents at seiche periods can contribute significantly to the flow; maximum currents at these periods can be as much as 10 times those caused by the M_2 tide, the largest tidal component in the harbour;

- low frequency currents driven by storms can lead to the strongest flows seen in the harbour; the low frequency events can cause circulation patterns that have near-surface outflow and deeper inflow or vice versa;

- sediment transport modelling of the strongest event seen in the current records led to net sediment displacement towards the head of the model harbour; mean circulation patterns from the existing data would also support net movement towards the head. There is some support for this physical result from existing distributions of pollutants in bottom sediments.

6. Acknowledgements

Sylvain de Margerie hunted through the ASA archives and provided us with the ADCP data from 1993, and the current meter and CTD data from 1992. Mark MacNeil helped to resolve the scaling problem with the 1993 ADCP data. TSRI provided funding to review the existing data from Sydney Harbour and to conduct the field program. Tim Milligan, with the assistance of Andrew Stuart and Brent Law, provided us with early access to the critical stress estimates for sediment resuspension in the harbour. This stimulated us to modify the formalism that determines the suspended fraction within the bblt model. Phillip Yeats and Donald Lawrence provided helpful internal reviews. We thank these individuals and the funding agency for their support.

7. References

ASA 1994. Industrial Cape Breton Receiving Water Study, Phase II, Vol. III, Data Report. 54 PP + 6 appendices.

Easton, A. K. 1972. Seiches in Sydney Harbour, N. S. Can. J. Earth Sci. 9, 857-862.

Ernst, B., D. Pitcher, S. Matthews and G. Julien 1999. Concentration and distribution of polycyclic aromatic hydrocarbons (PAHs), PCBs, and metals in sediments, mussels (Mytilus edulis and Modiolus modiolus), and lobsters (homarus americanus) from Sydney Harbour, Nova Scotia. Environment Canada, Environmental Protection Branch, Surveillance Report EPS-5-AR-99-7, Dartmouth, Canada, 30 pp.

Gregory, D., B. Petrie, F. Jordan and P. Langille 1993. Oceanographic, geographic and hydrological parameters of Scotia-Fundy and southern Gulf of St. Lawrence inlets. Can. Tech. Rep. Hydrogr. Ocean Sci. 143, 248 pp.

Hannah, C., Y. Shen, J. Loder and K. Muschenheim. 1995. bblt - Formulation and exploratory applications of a benthic boundary layer transport model. Can. Tech. Rep. Hydrogr. Ocean Sci. 166, 58 pp.

Honda, K. and W. B. Dawson. 1911. On the secondary undulations of the Canadian tides. Sci. Rep. Tohuku Univ., Japan, 1, 61-66.

Lane, P. A. 1988. Carcinogen – circulation model for Sydney Tar Ponds. P. Lane and Associates Ltd., Halifax, N. S., 340 pp.

Petrie, B., K. Drinkwater, D. Gregory, R. Pettipas and A. Sandström 1996. Temperature and salinity atlas for the Scotian Shelf and the Gulf of Maine. Can. Tech. Rep. Hydrogr. Ocean Sci. 171, 398 pp.

Tedford, T., E. Gonzalez and C. Hannah 2001. bblt Version 3.1 User's Manual. Can. Tech. Rep. Hydrogr. Ocean Sci. 213, 48 pp.

Vandermeulen, J. H. 1989. PAH and heavy metal pollution of the Sydney Estuary: summary and review of studies to 1987. Can. Tech. Rep. Hydrogr. Ocean Sci. 108, 48 pp.

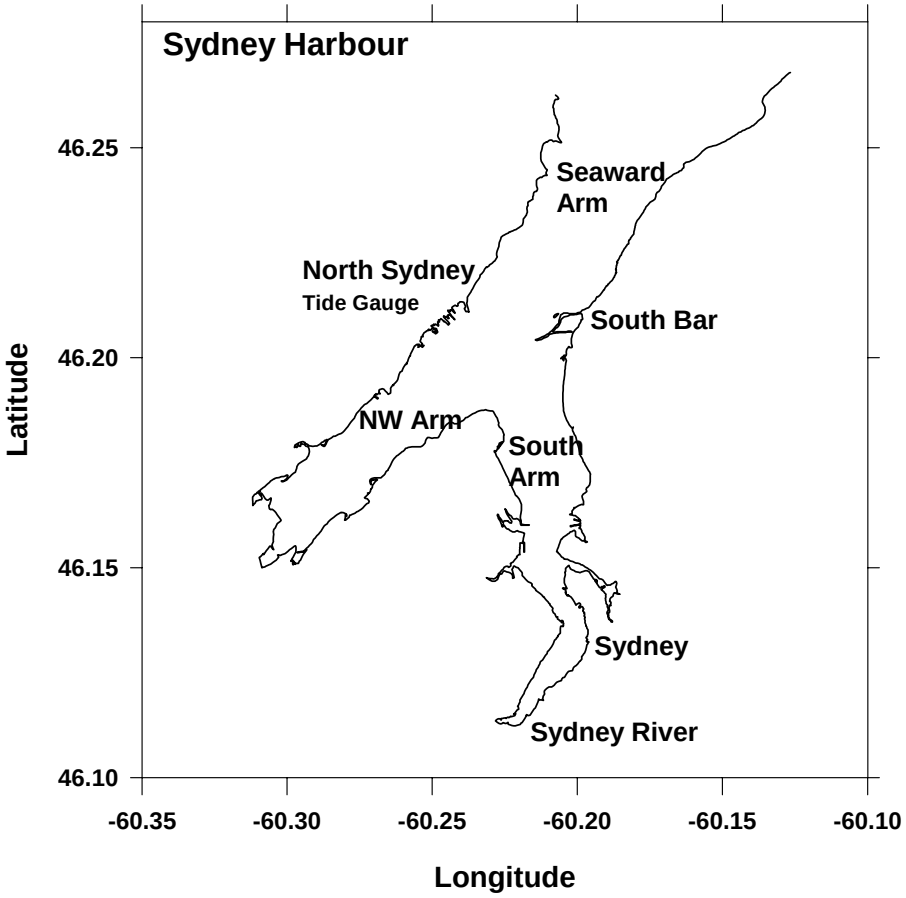

Figure 1. Base map of Sydney Harbour showing the separate arms.

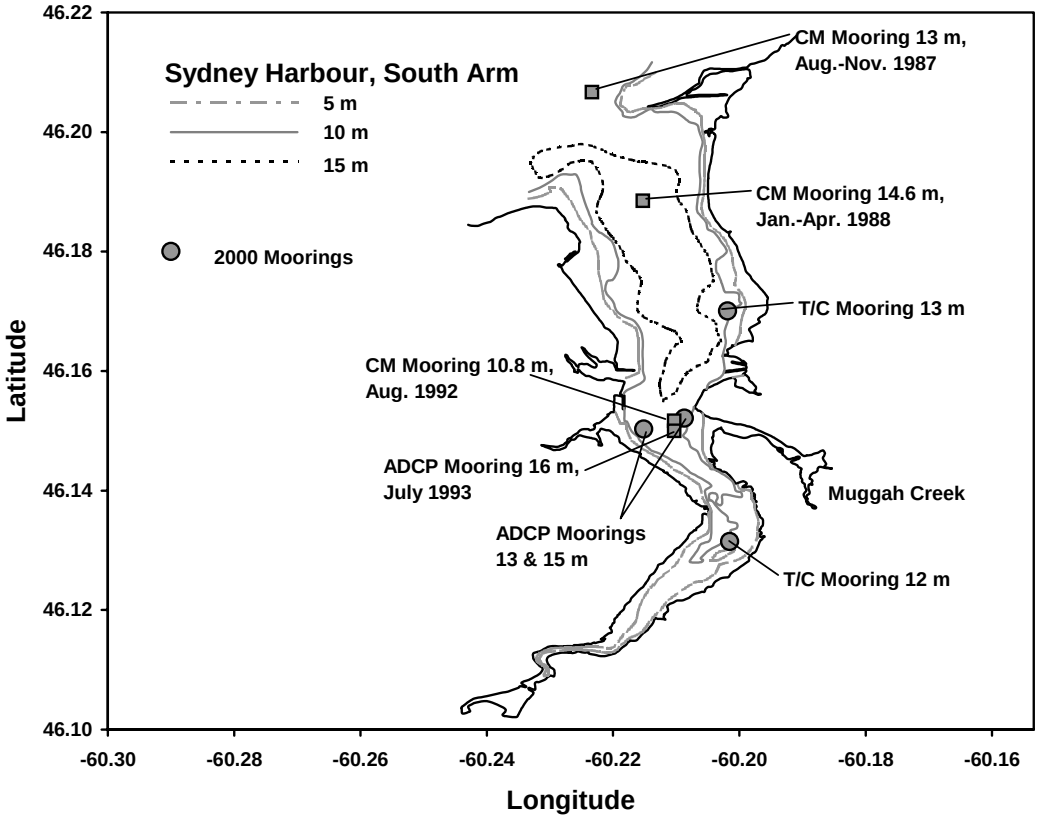

Figure 2. Location of mooring sites from the studies of Lane (1988), ASA (1994) and the current mooring program.

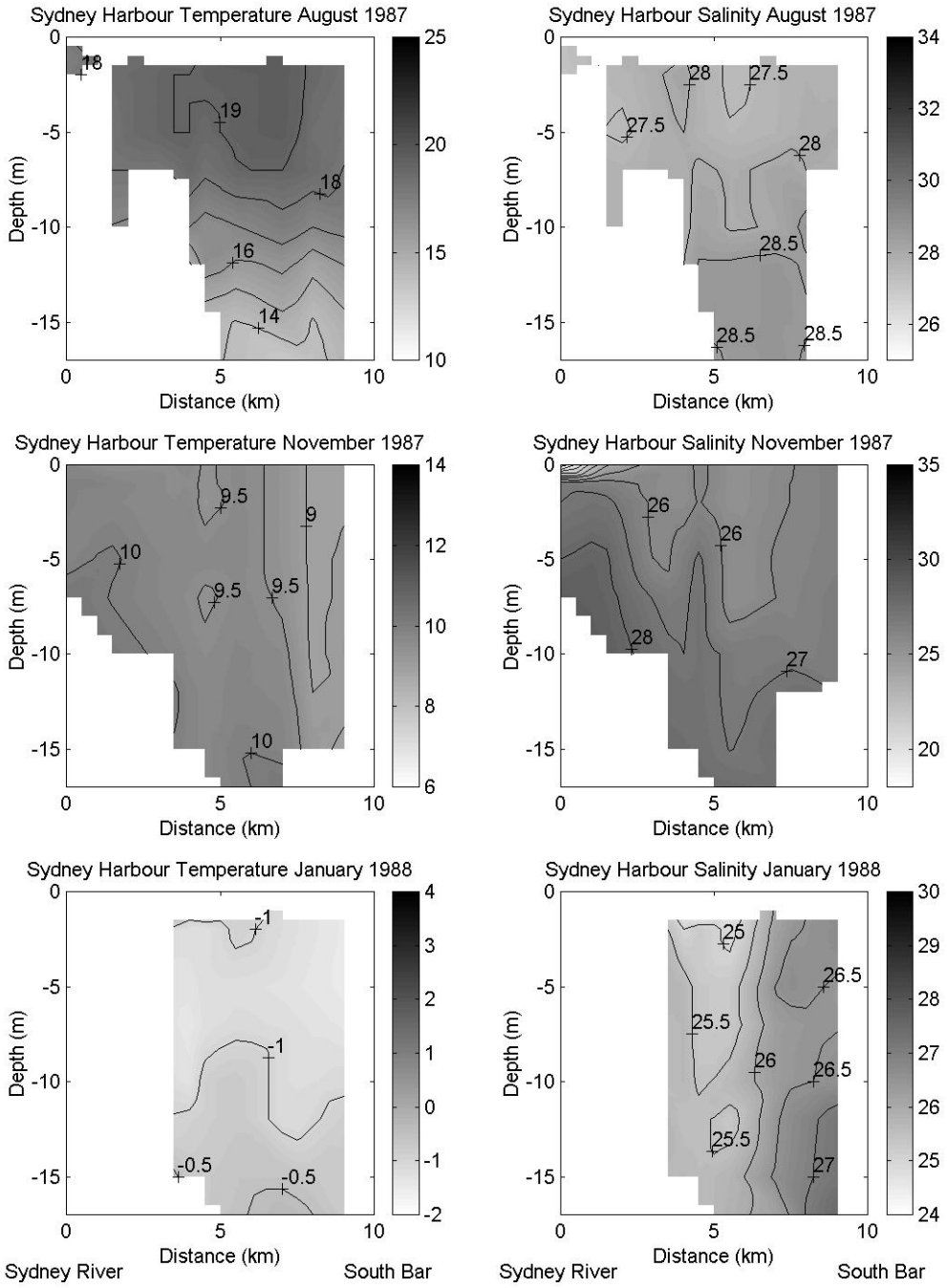

Figure 3. Temperature and salinity sections along the south arm of Sydney Harbour, redrawn from Lane (1988). Bottom depths are based on the depths of the observations.

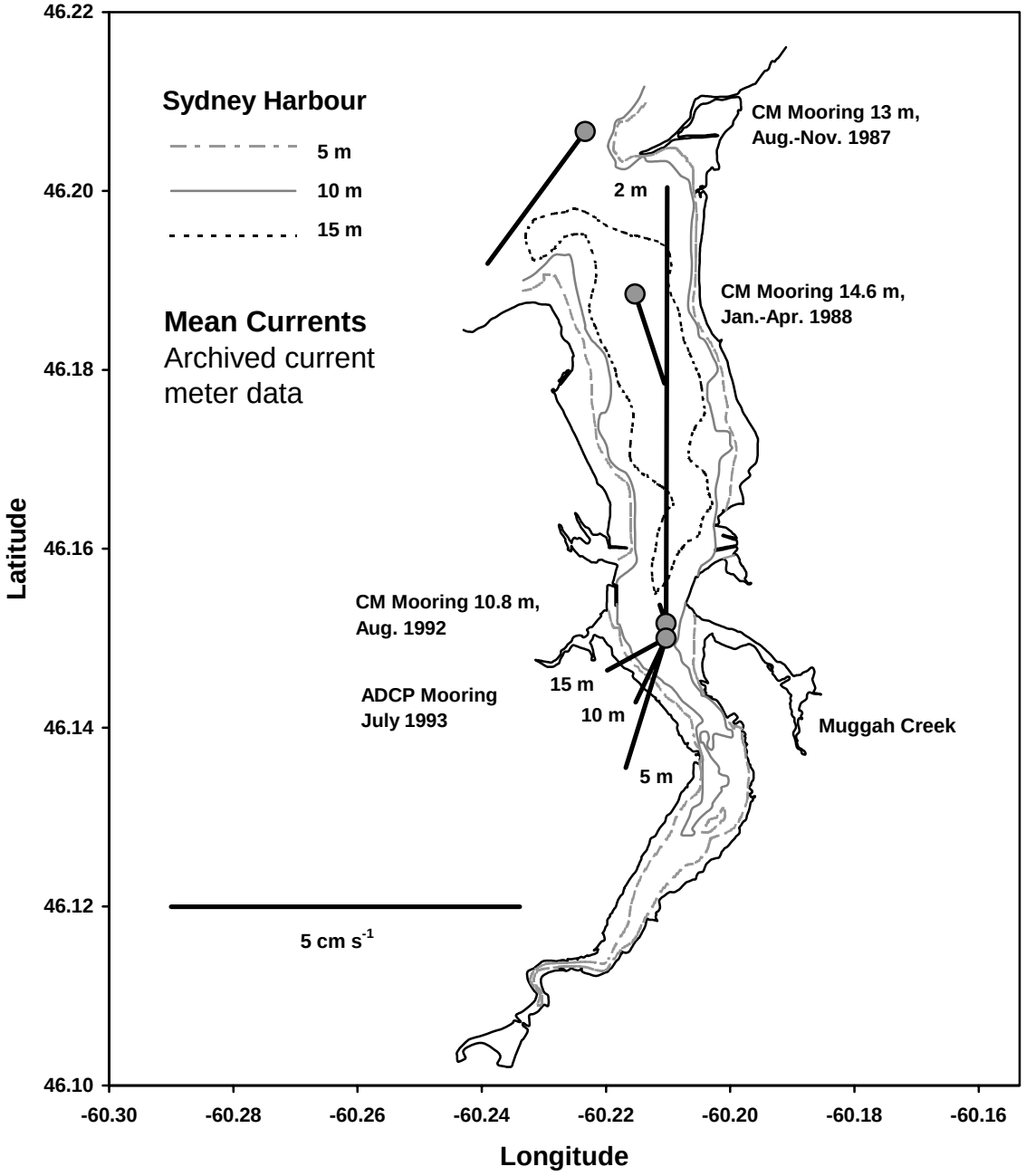

Figure 4. Mean current vectors from Lane (1988) and ASA (1994) deployments. Note that the numbers near the end of the ADCP vectors correspond to the depths of the observations.

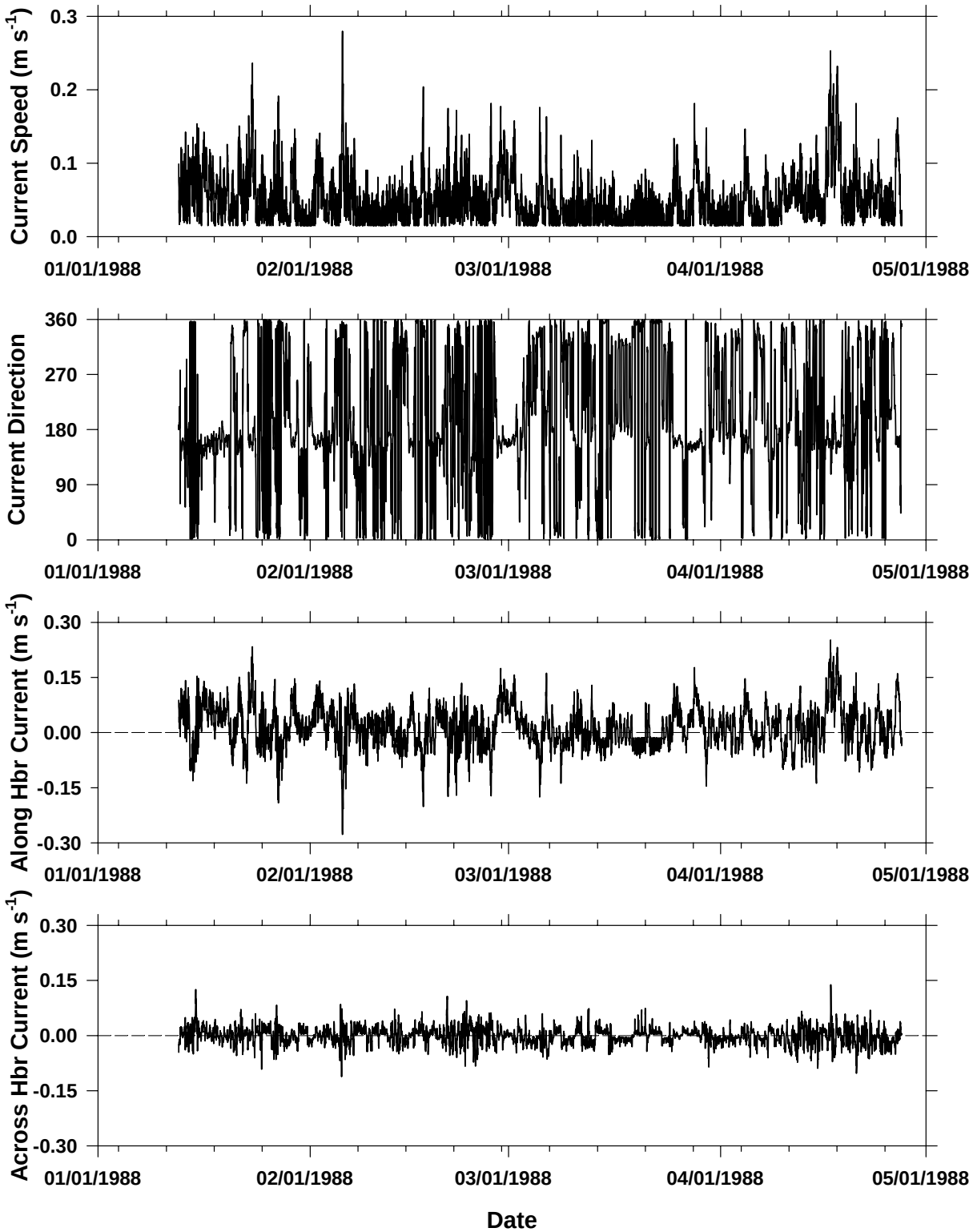

Figure 5. Time series of current speed (m s-1), direction, along-, and across-harbour current for the mooring located near the mouth of the south arm of Sydney Harbour, Jan.-Apr. 1988 (see Fig. 2).

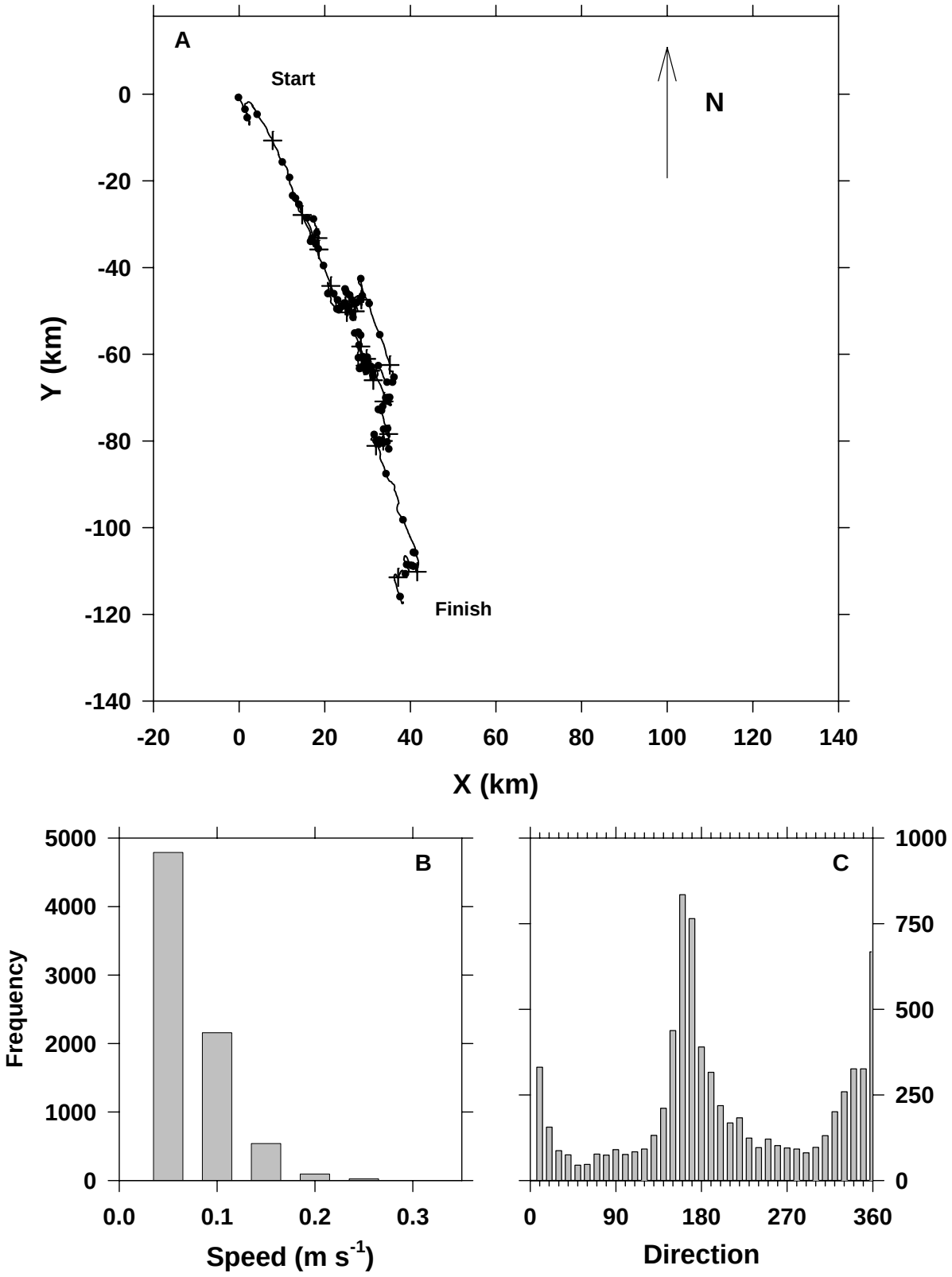

Figure 6. (A) Progressive vector diagram for the Jan.-Apr. 1988 current meter record. Solid dots mark 00:00 of each day, crosses every 5th day. Histograms of current **(B)** speed and **(C)** direction.

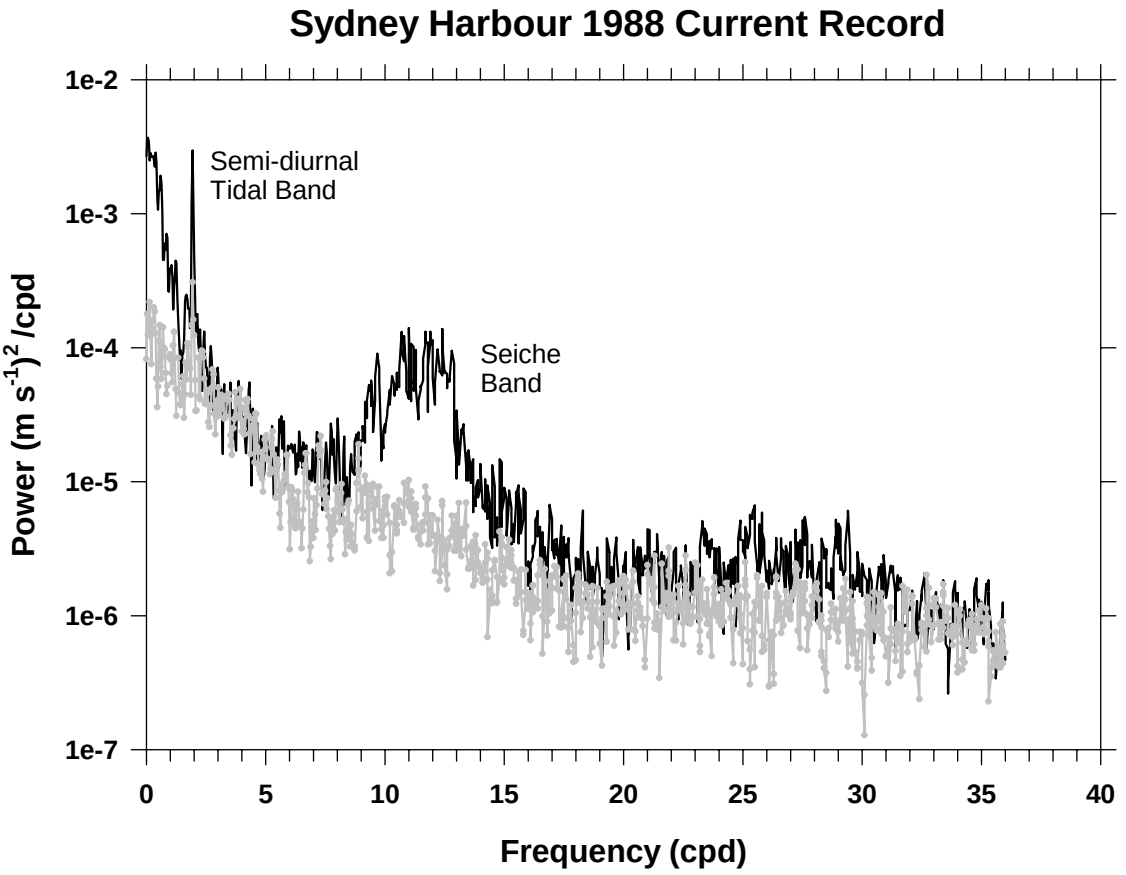

Figure 7. Spectra of along- (black line) and across- (grey line and dots) harbour current from the Jan.-Apr. 1988 mooring located near the mouth of the south arm of Sydney Harbour.

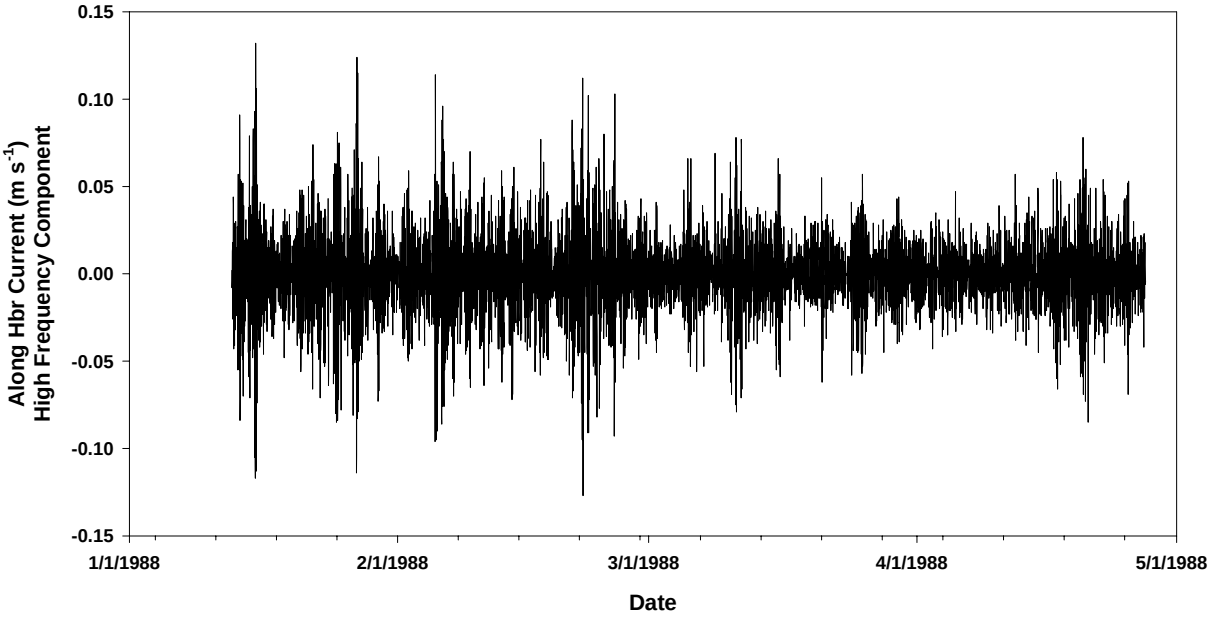

Figure 8. Along-harbour component of current, filtered to pass the high freqency flows.

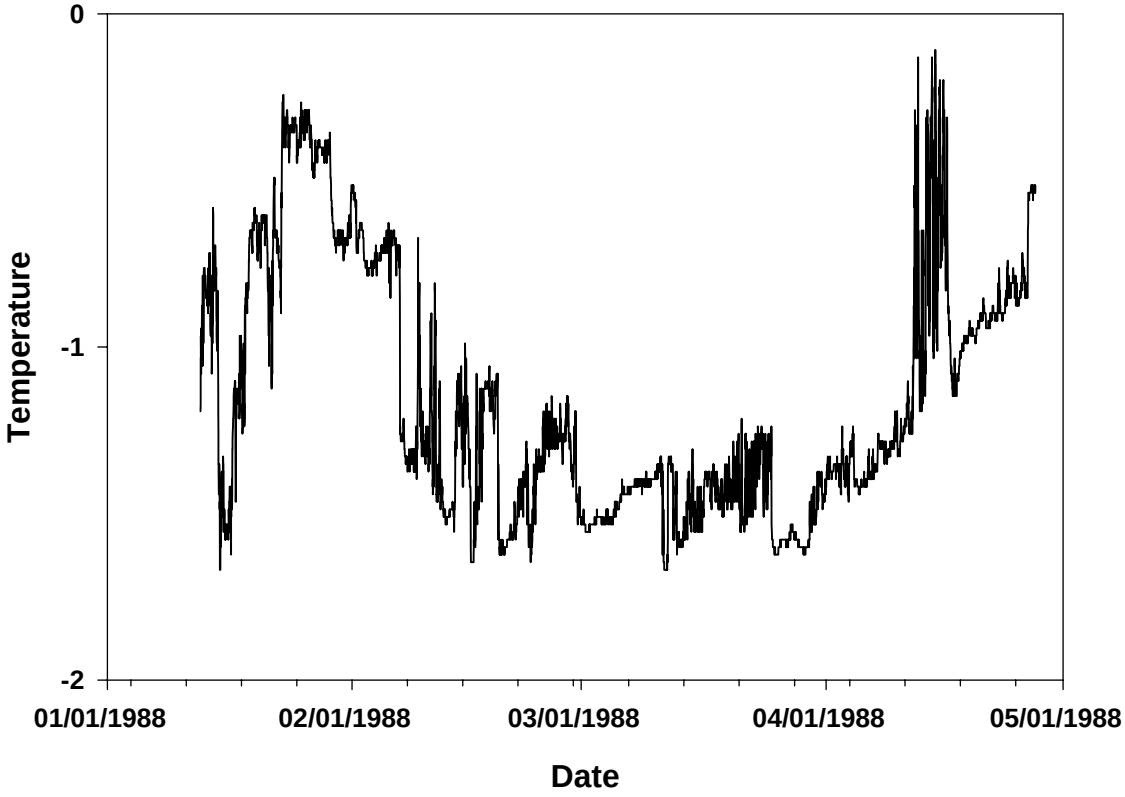

Figure 9. Temperature from the current meter moored near the mouth of the south arm of Sydney Harbour, Jan.-Apr. 1988.

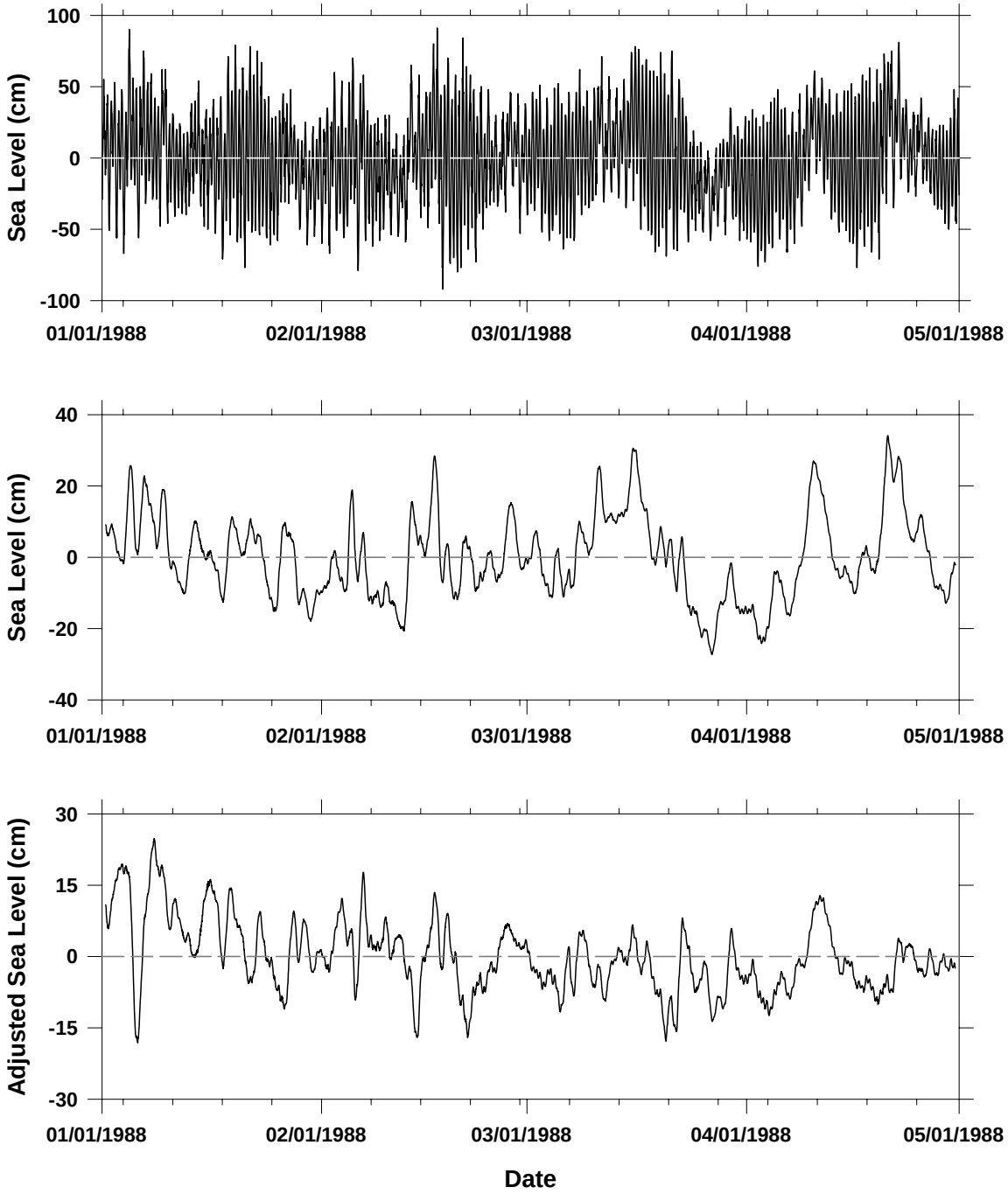

Figure 10. (A) Sea level, **(B)** filtered sea level and **(C)** adjusted sea level after processing with a 25 h running mean filter. Data are from the North Sydney tide gauge (see Fig. 1).

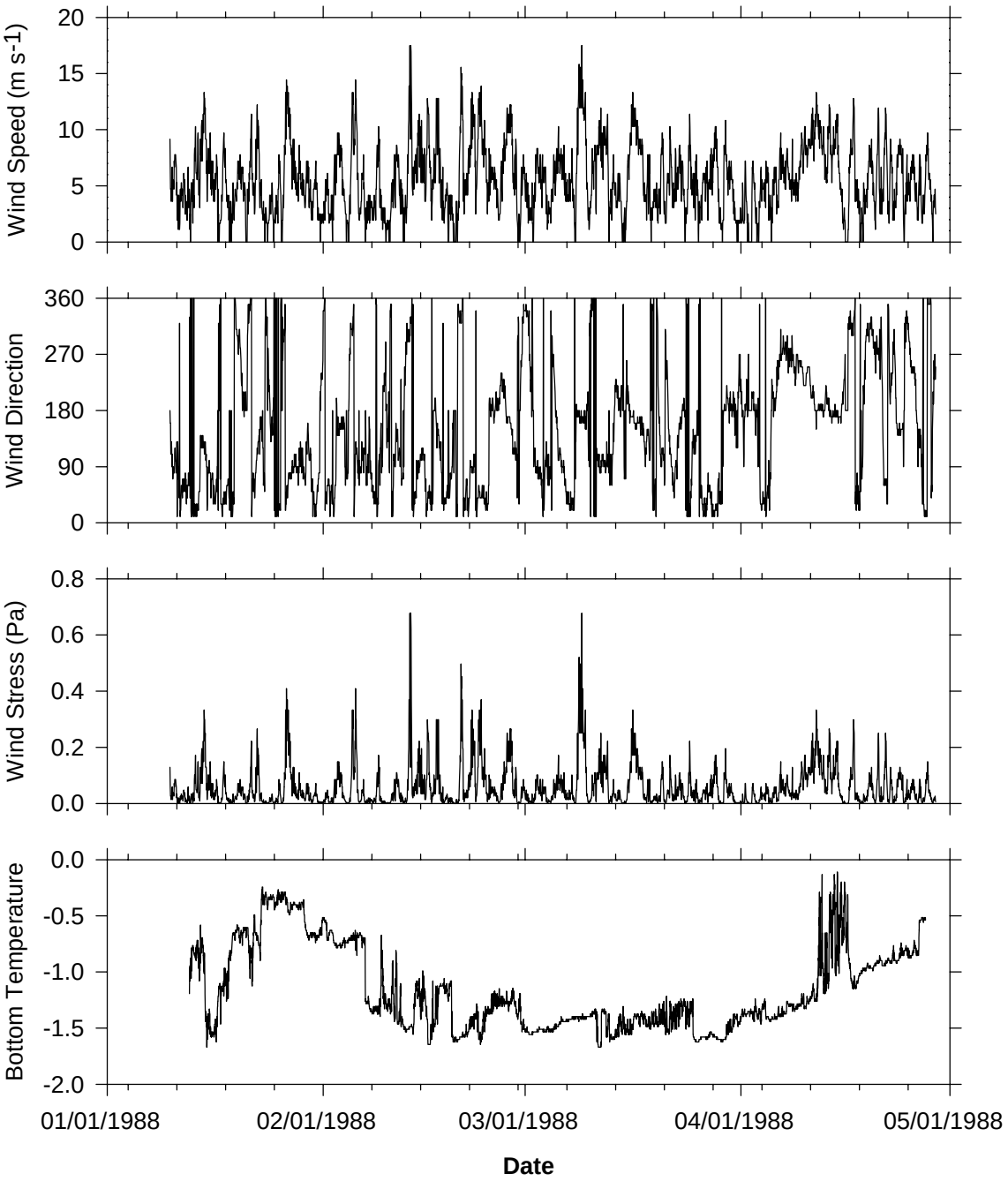

Figure 11. Wind speed, direction (direction to) and wind stress from Sydney Airport. Temperature from the Jan.-Apr. 1988 current meter near the mouth of the south arm of Sydney Harbour.

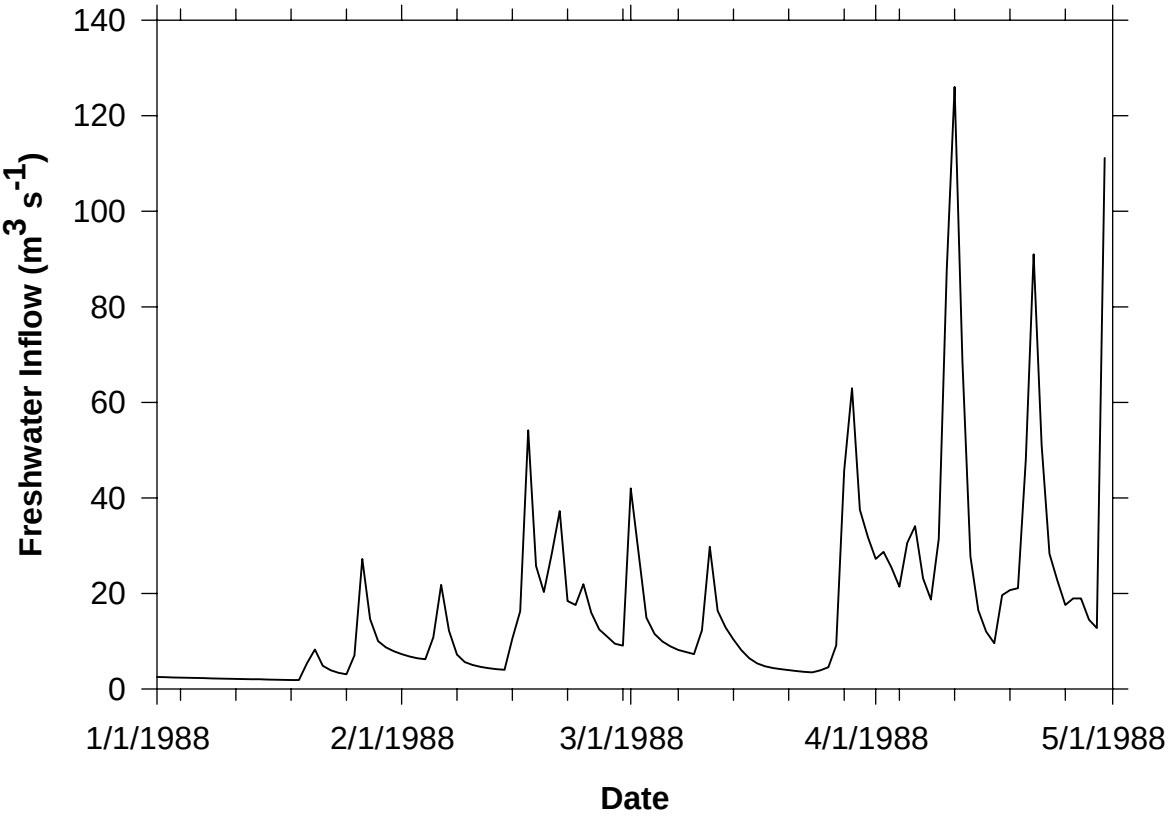

Figure 12. Estimated freshwater flow ($m^3\ s^{-1}$) into Sydney Harbour.

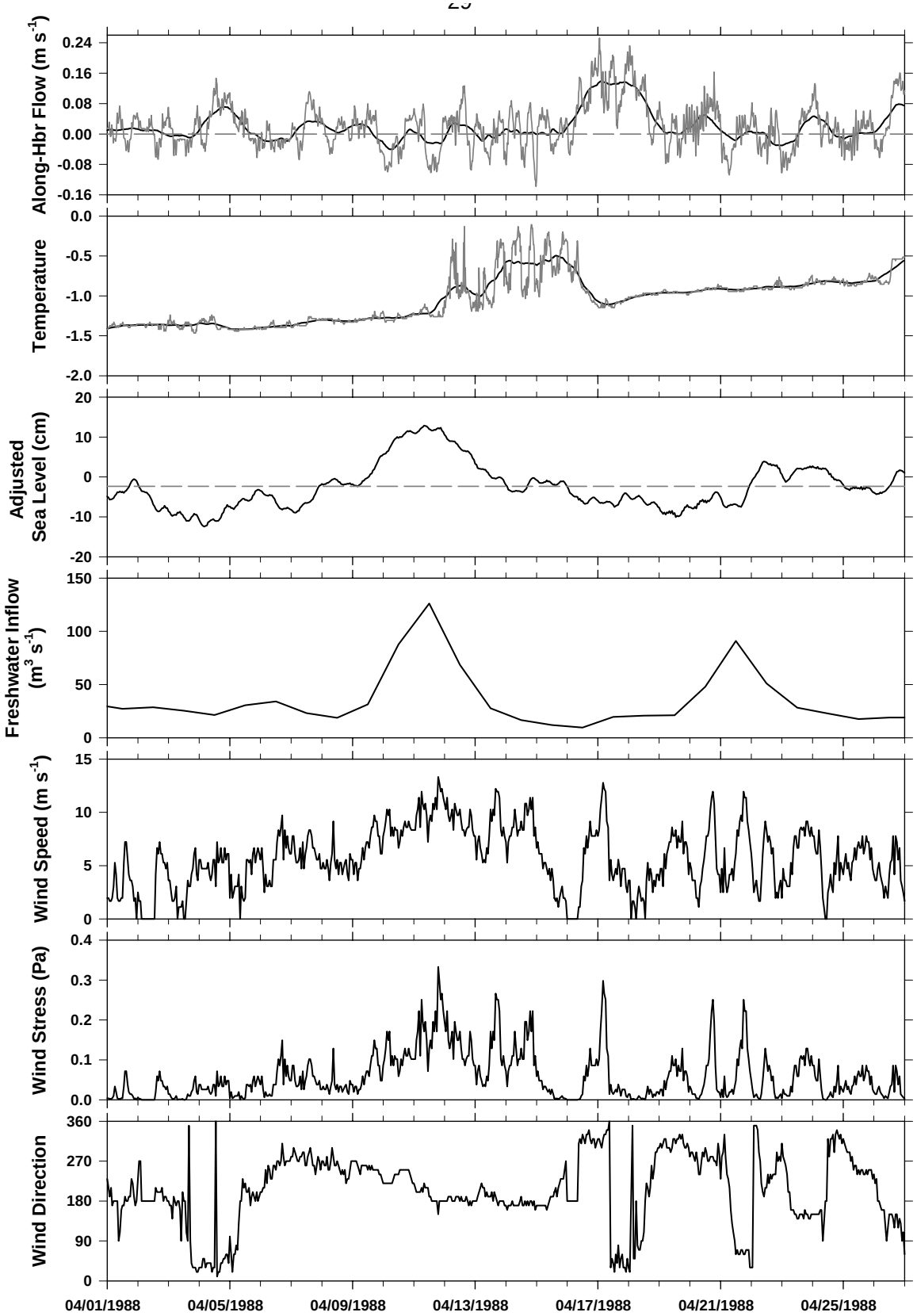

Figure 13. Along-harbour flow and temperature (raw and filtered), adjusted sea level, freshwater inflow, wind speed, stress and direction are shown for April 1988. The reference line for adjusted sea level is its April mean.

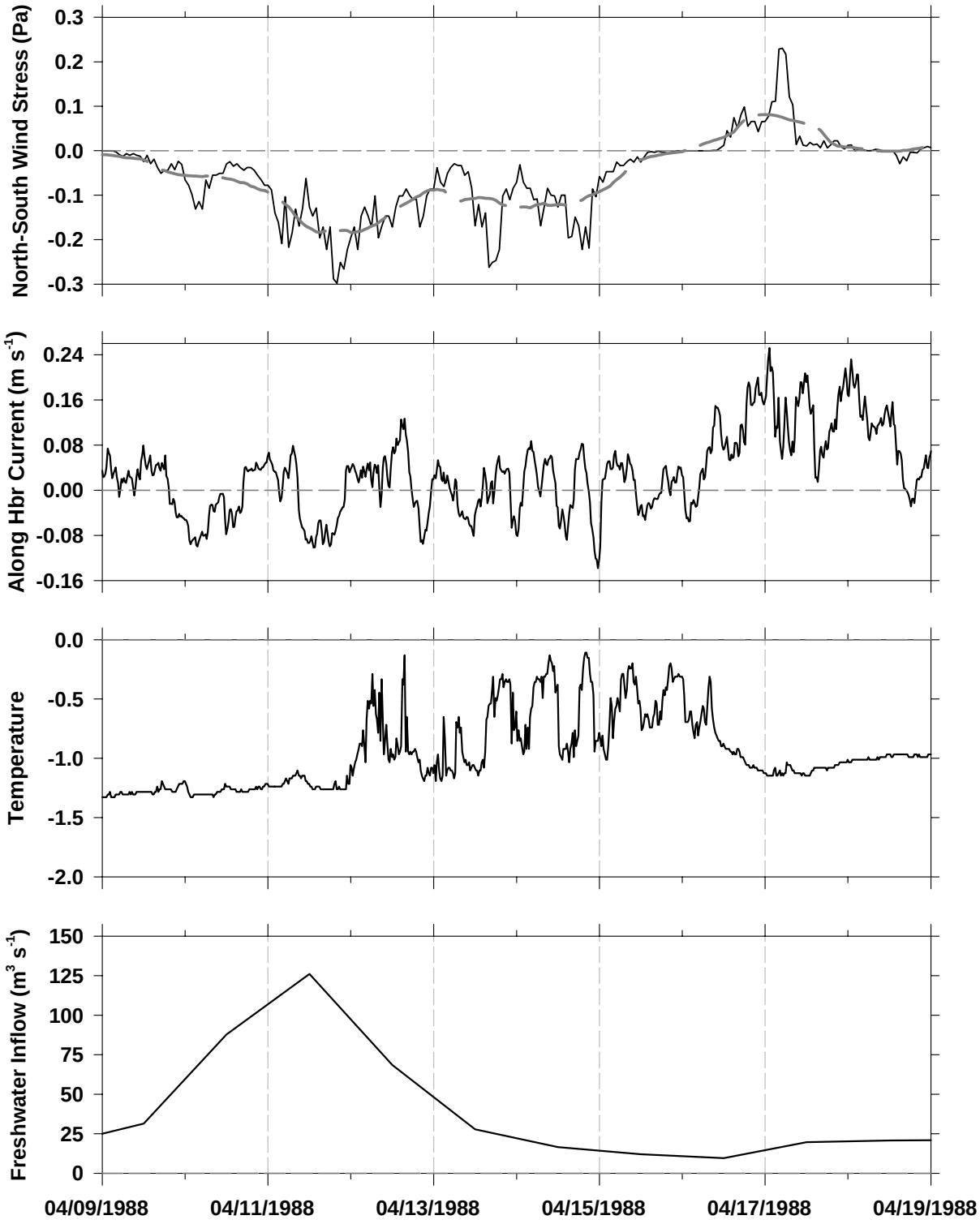

Figure 14. Time series of north-south wind stress (positive northwards, 25 h RMF also shown), along-harbour current (positive into the harbour), temperature and freshwater inflow.

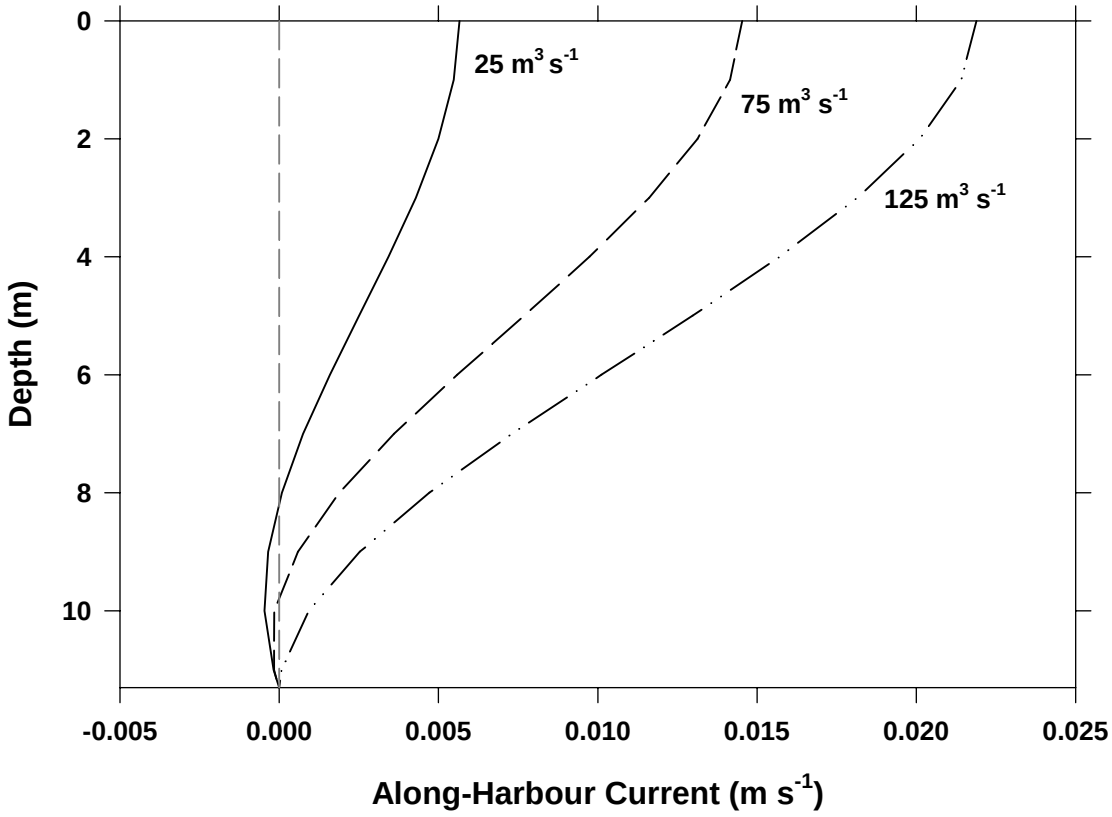

Figure 15. Along-harbour currents from the Hansen-Rattray solutions for 25, 75, and 125 $m^3\ s^{-1}$ freshwater inflow, zero wind stress.

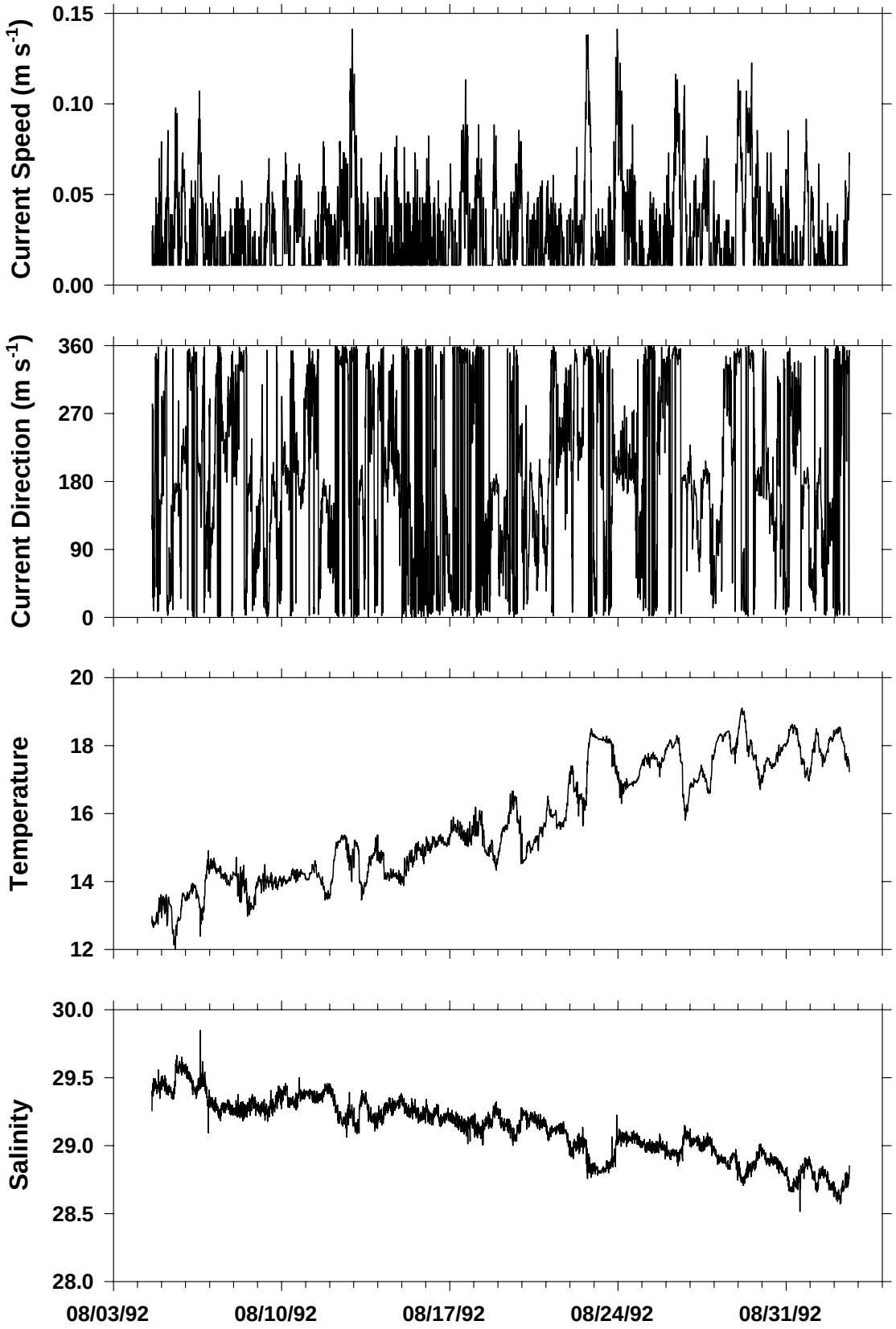

Figure 16. Current speed, direction, temperature and salinity time series from instrument moored in Sydney Harbour August-September 1992 (ASA 1994).

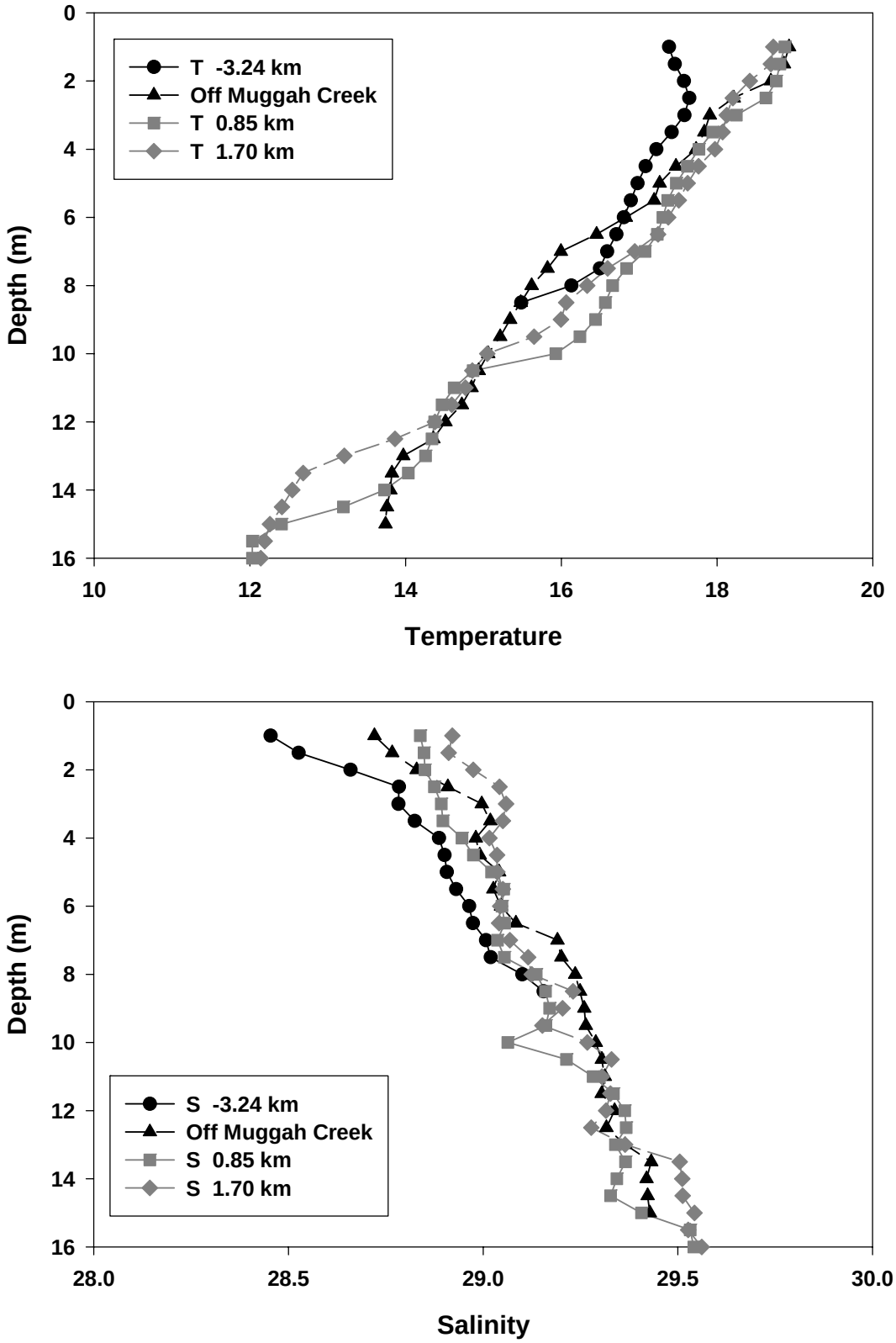

Figure 17. Temperature and salinity profiles from Sydney Harbour, August 20 1992. Distances are relative to station off the mouth of Muggah Creek, negative (positive) towards the head (mouth).

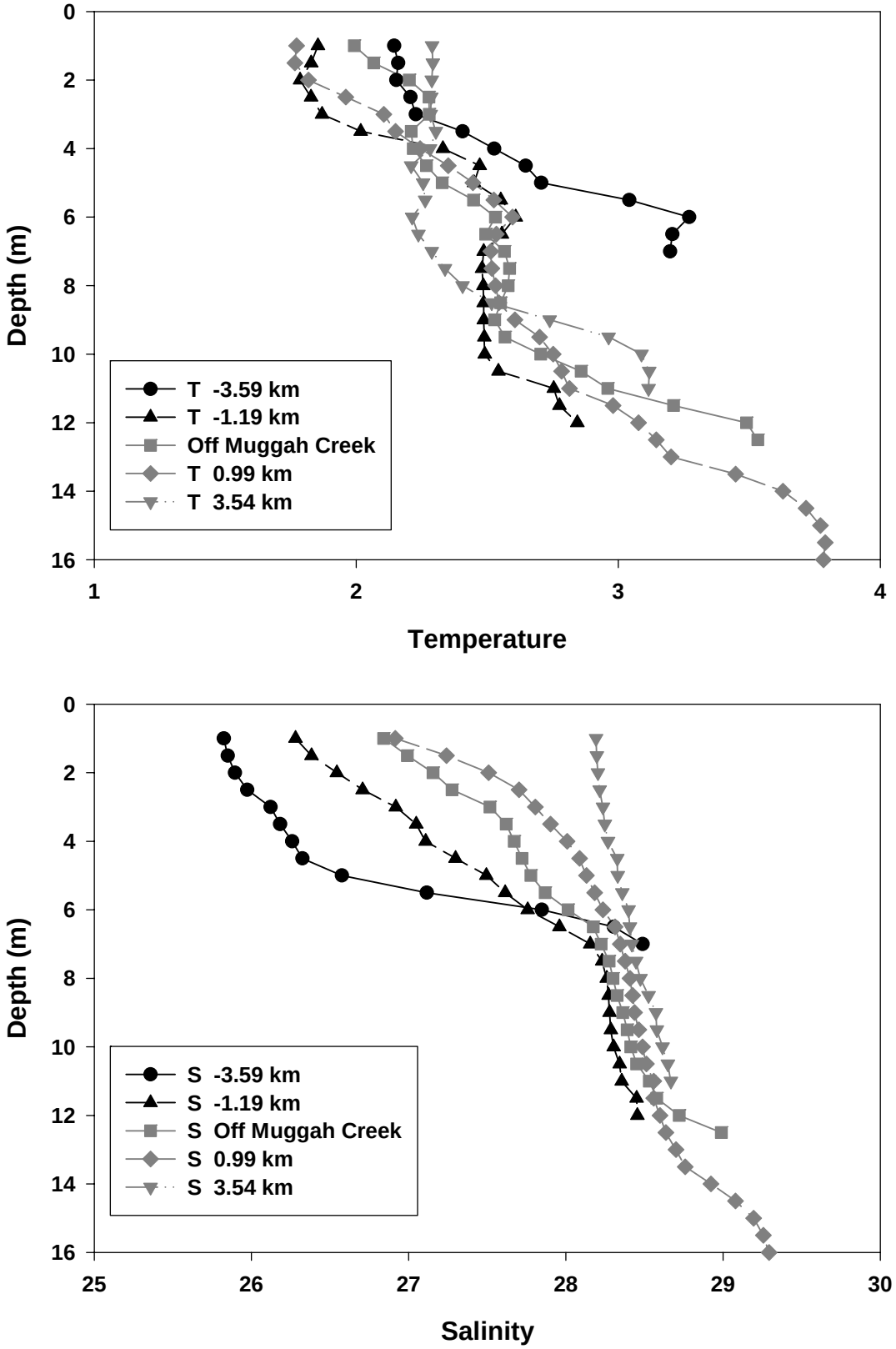

Figure 18. Temperature and salinity profiles from Sydney Harbour, December 16 1992. Distances are relative to station off the mouth of Muggah Creek, negative (positive) towards the head (mouth).

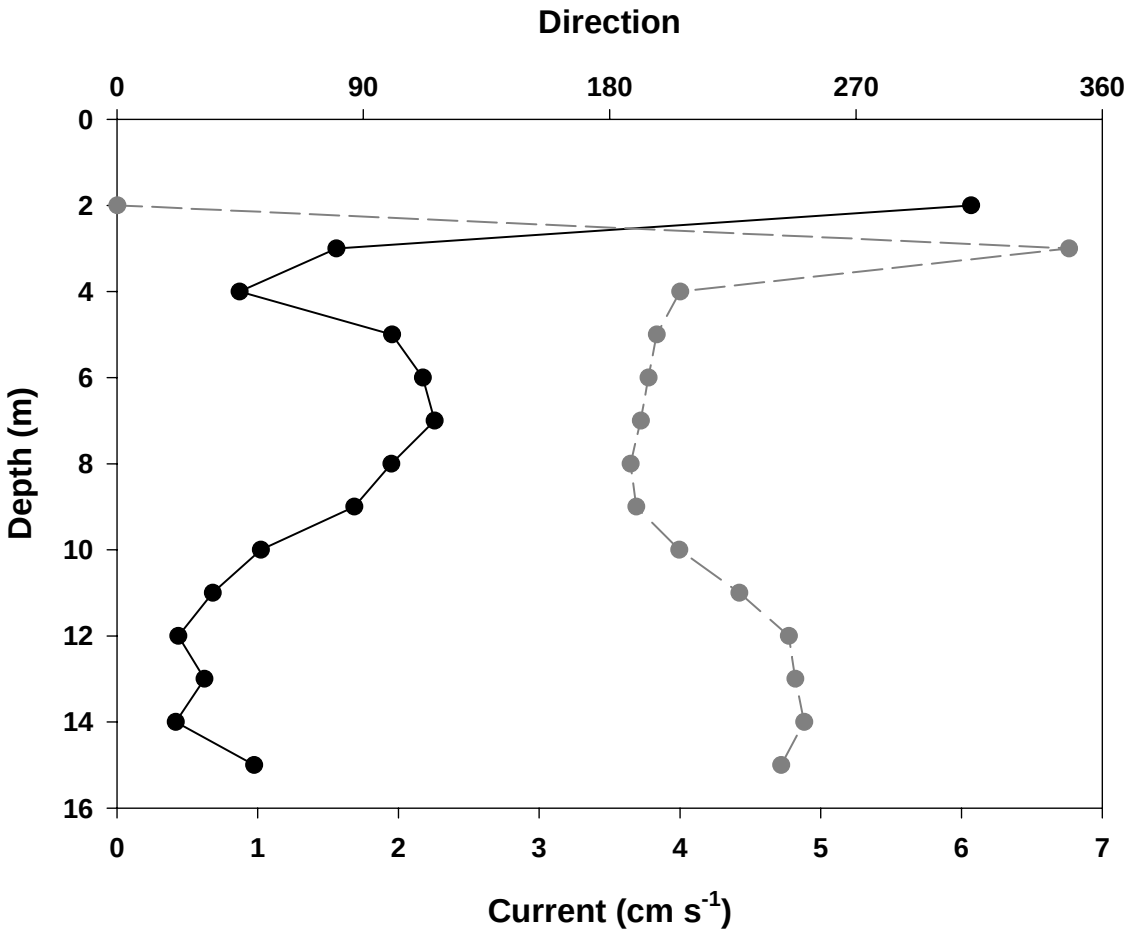

Figure 19. Mean current speed (solid line, black dot) and direction (broken line, grey dot) for 1993 ADCP mooring off Muggah Creek (ASA 1994).

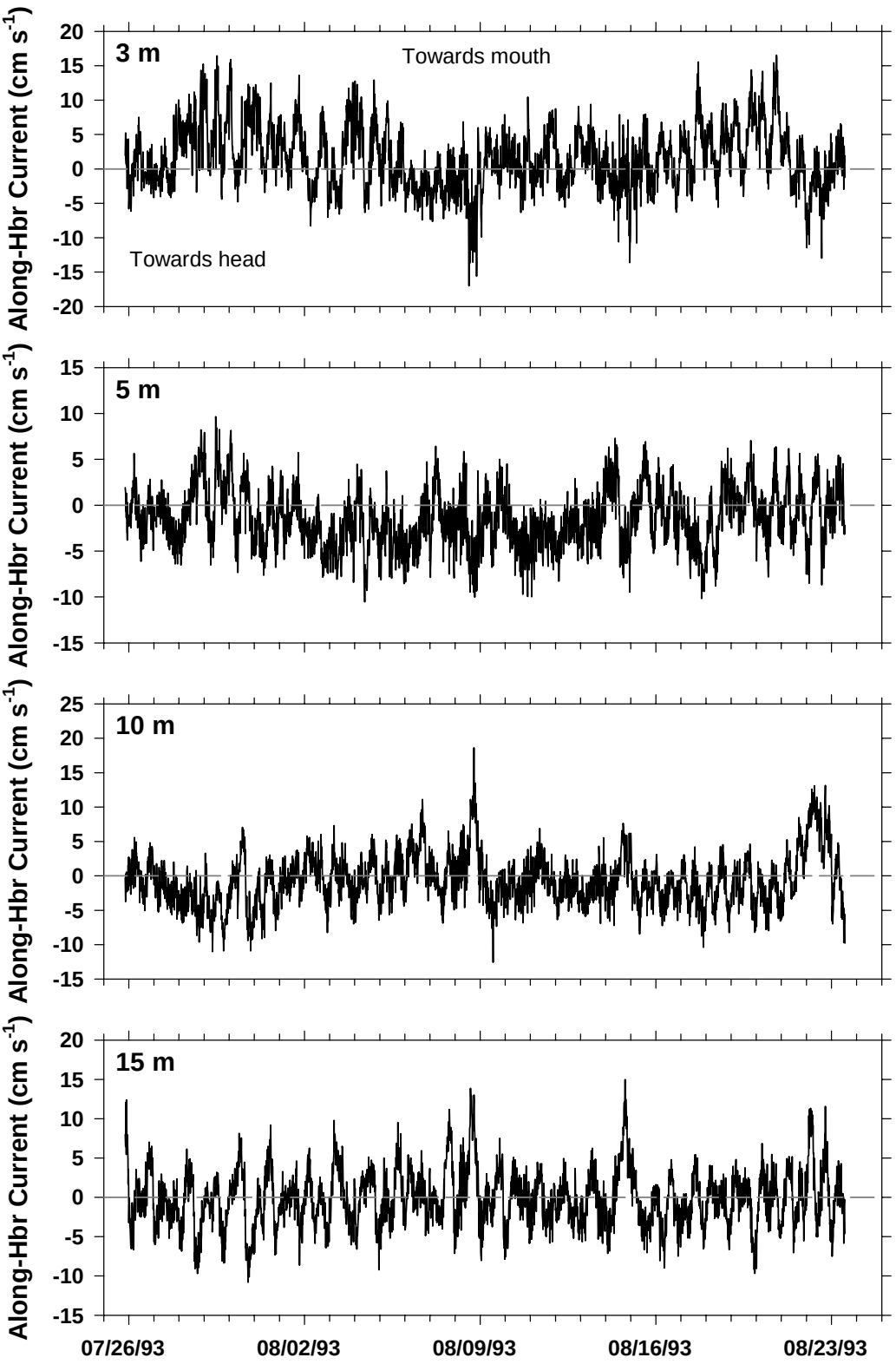

Figure 20. Time series of along-harbour current (along 337^{o}) at selected depths from ADCP mooring off Muggah Creek, 1993 (ASA 1994).

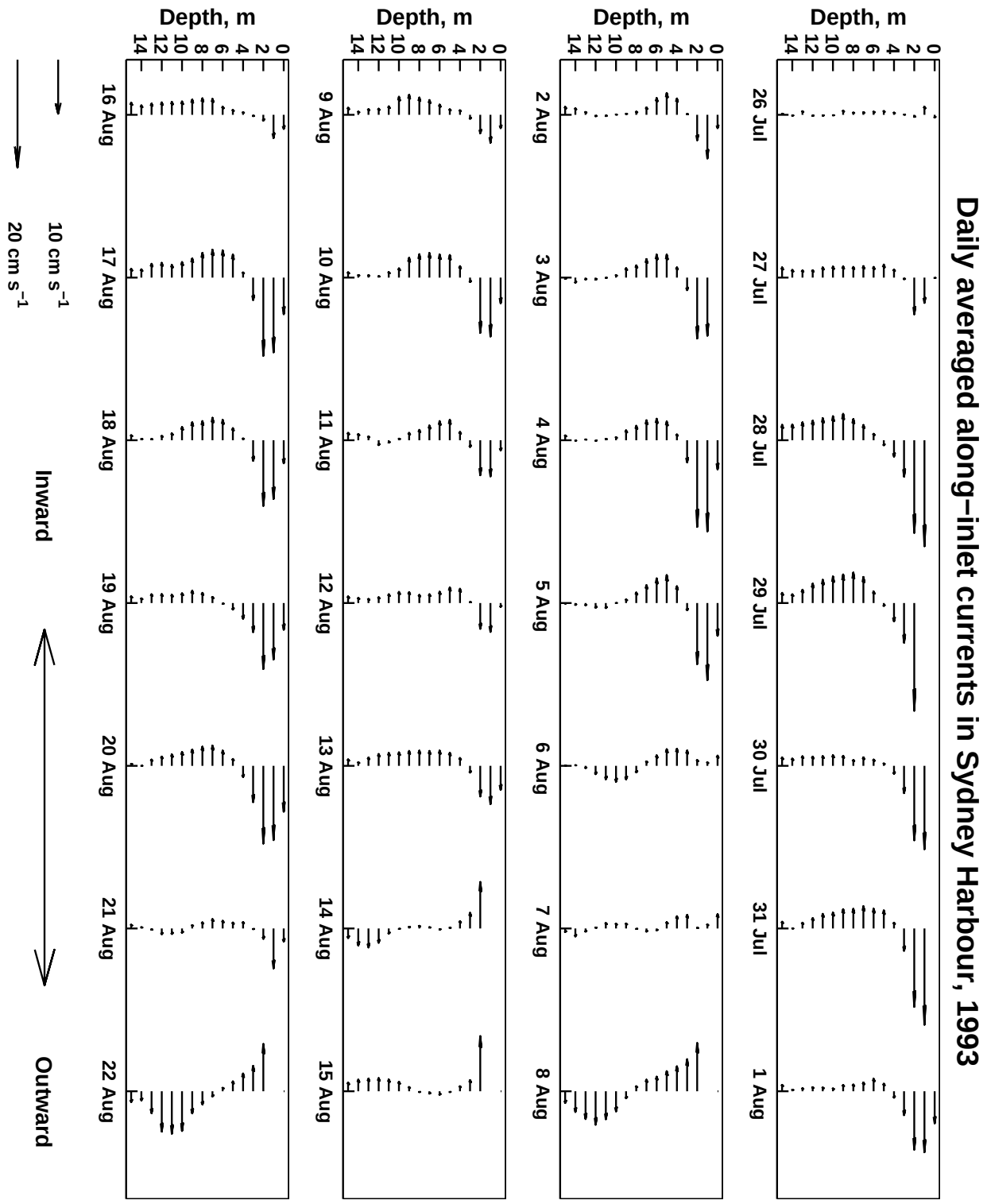

Figure 21. Daily mean current profiles from ADCP mooring off Muggah Creek, July-August 1993 (ASA 1994).

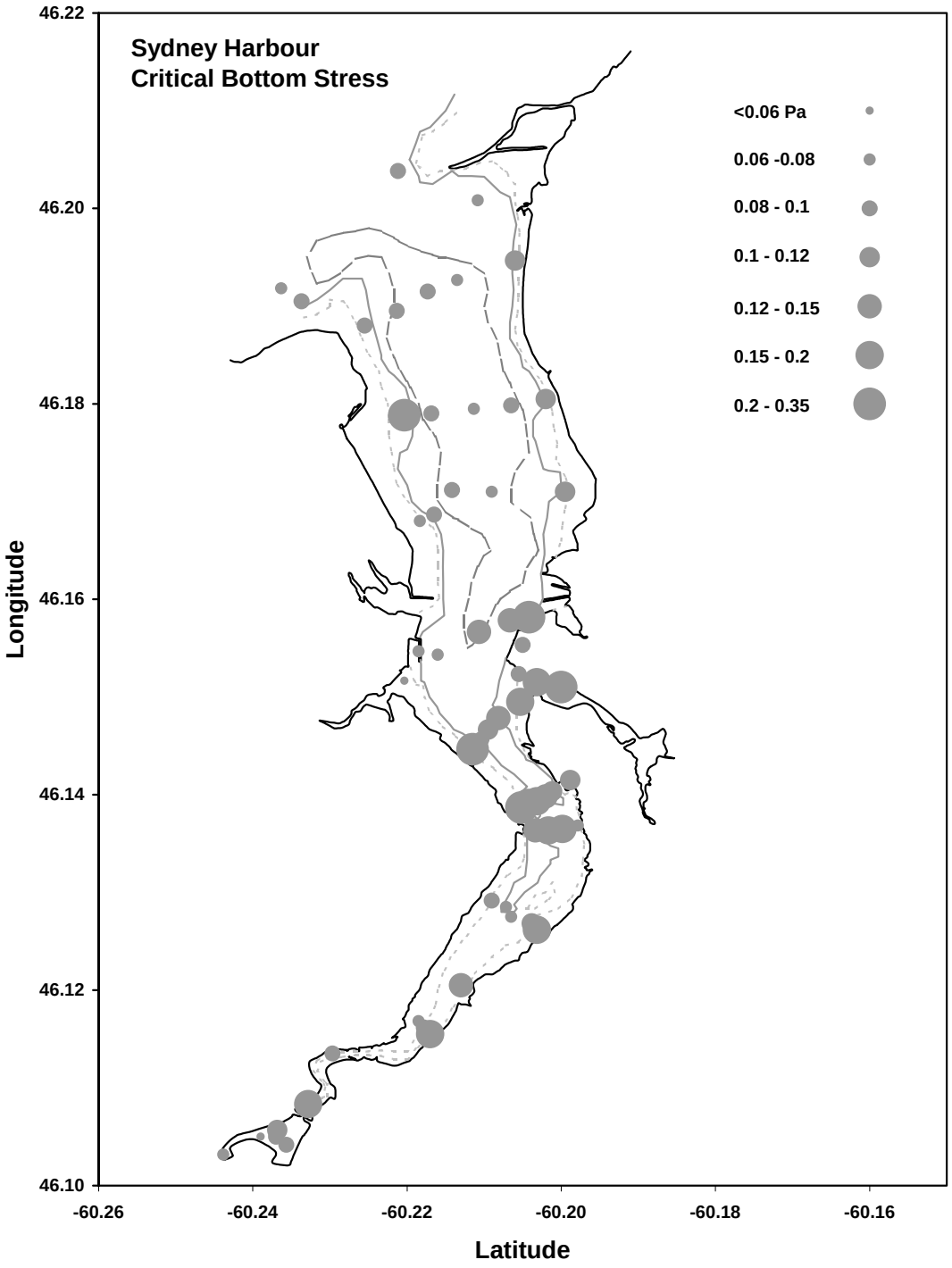

Figure 22. Critical bottom stresses for Sydney Harbour estimated from size distribution of bottom sediments (courtesy of T. Milligan, Marine Environmental Sciences Division, DFO, Dartmouth N. S.).

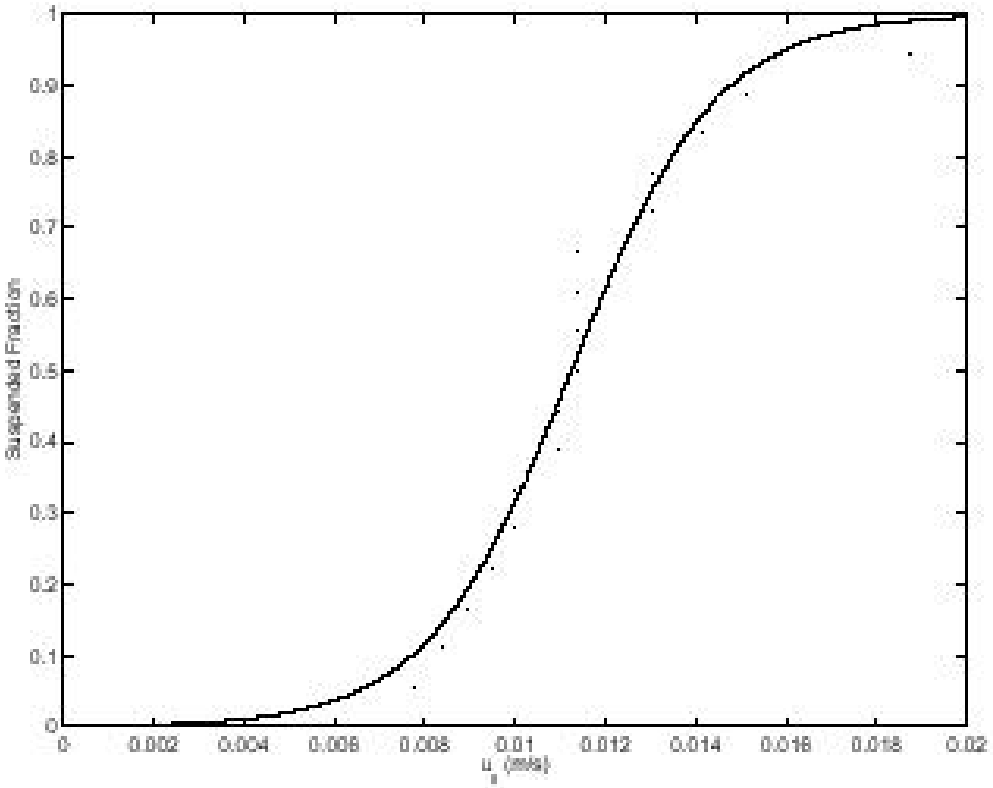

Figure 23. Fraction of suspended sediment as a function of friction velocity for Sydney Harbour. Critical bottom stress computations that allowed estimates of the friction velocity are courtesy of T. Milligan and co-workers, Marine Environmental Sciences Division, DFO, Dartmouth, N. S.

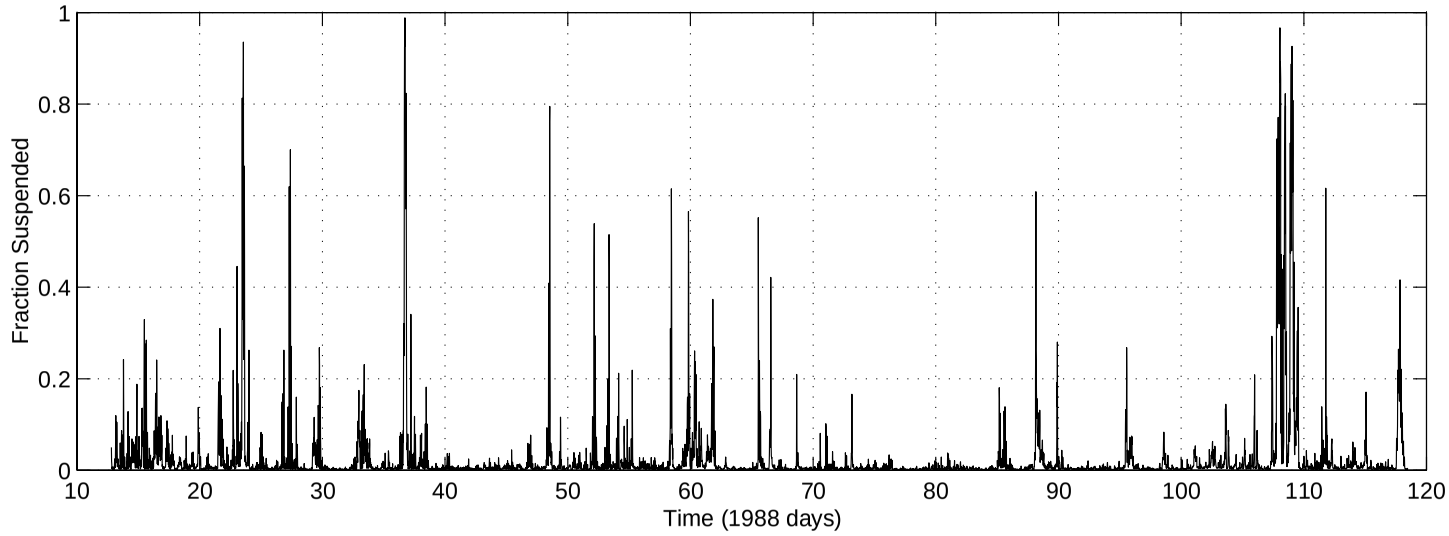
Fraction Suspended
0
0.2
0.4
0.6
0.8
1
10
20
30
40
50
60
70
80
90
100
110
120
Time (1988 days)

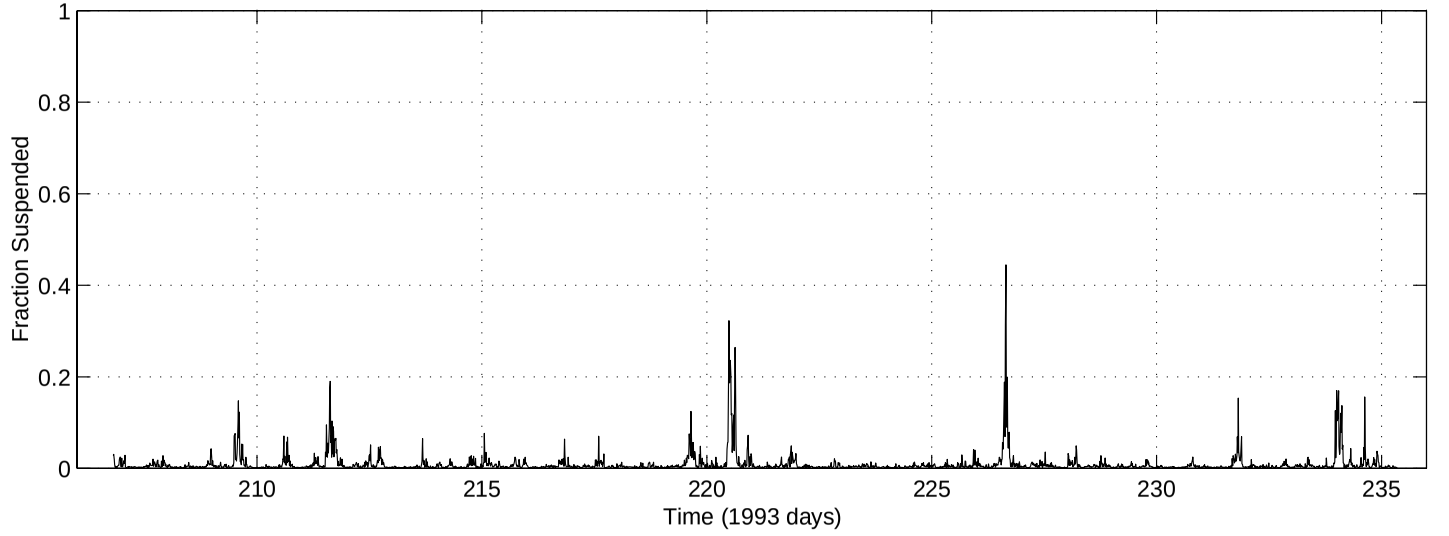
Fraction Suspended
0
0.2
0.4
0.6
0.8
1
210
215
220
225
230
235
Time (1993 days)

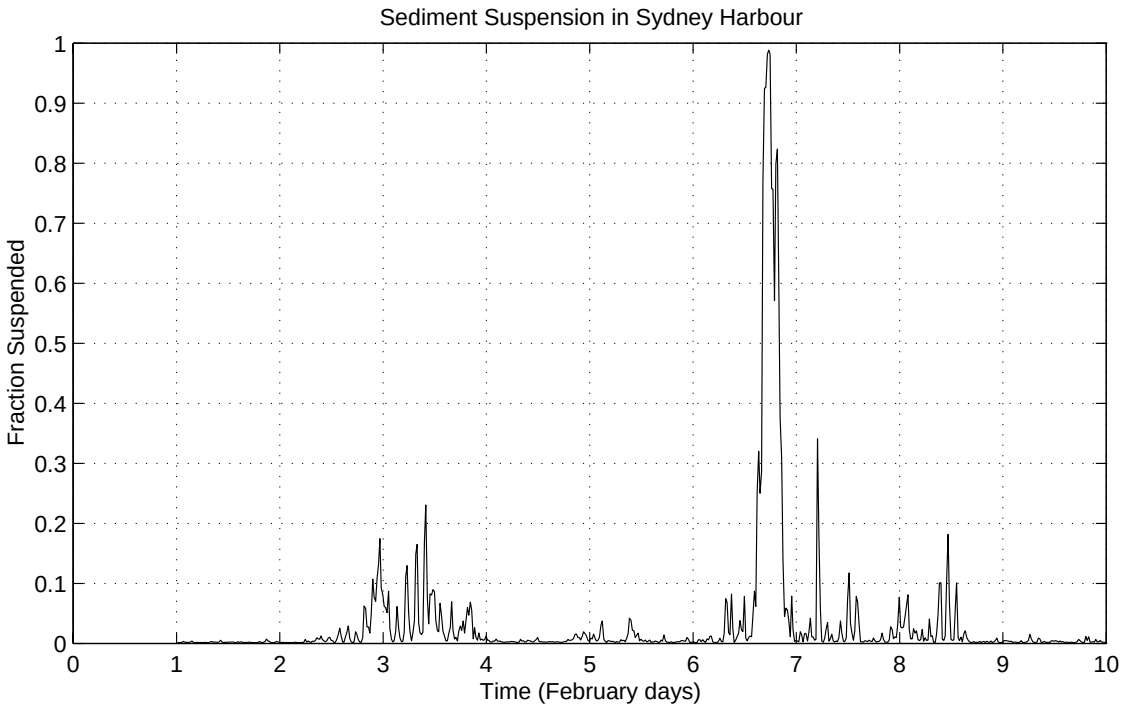
Sediment Suspension in Sydney Harbour
Fraction Suspended
Time (February days)
0
0.1
0.2
0.3
0.4
0.5
0.6
0.7
0.8
0.9
1
0
1
2
3
4
5
6
7
8
9
10

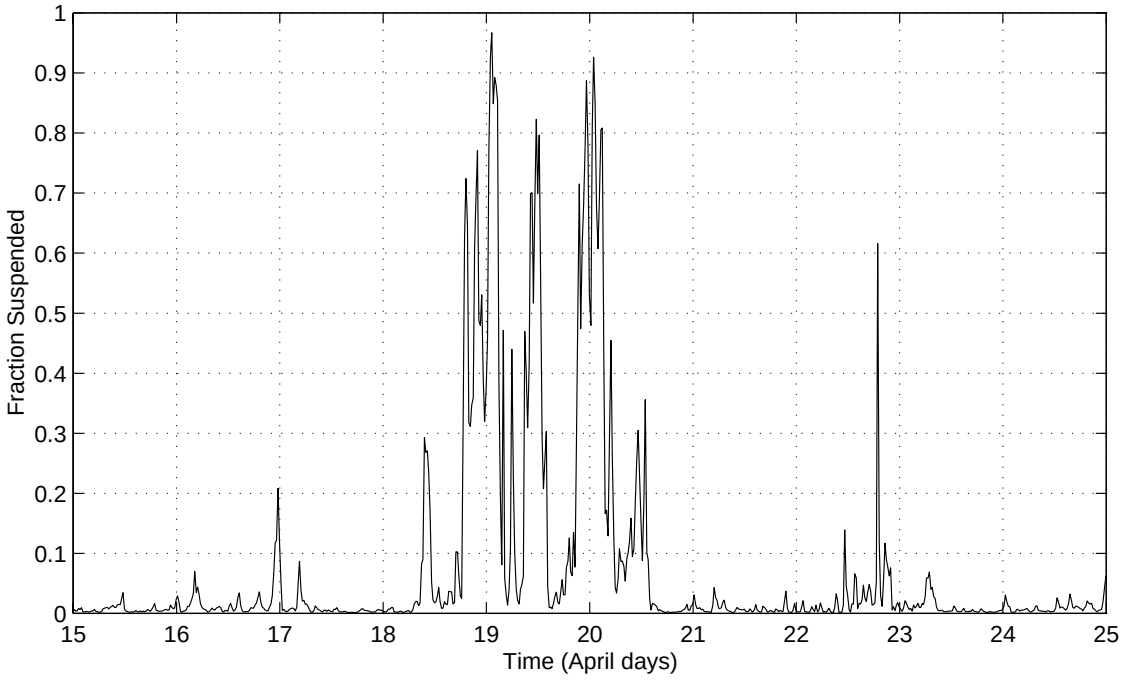
Fraction Suspended
Time (April days)
0
0.1
0.2
0.3
0.4
0.5
0.6
0.7
0.8
0.9
1
15
16
17
18
19
20
21
22
23
24
25

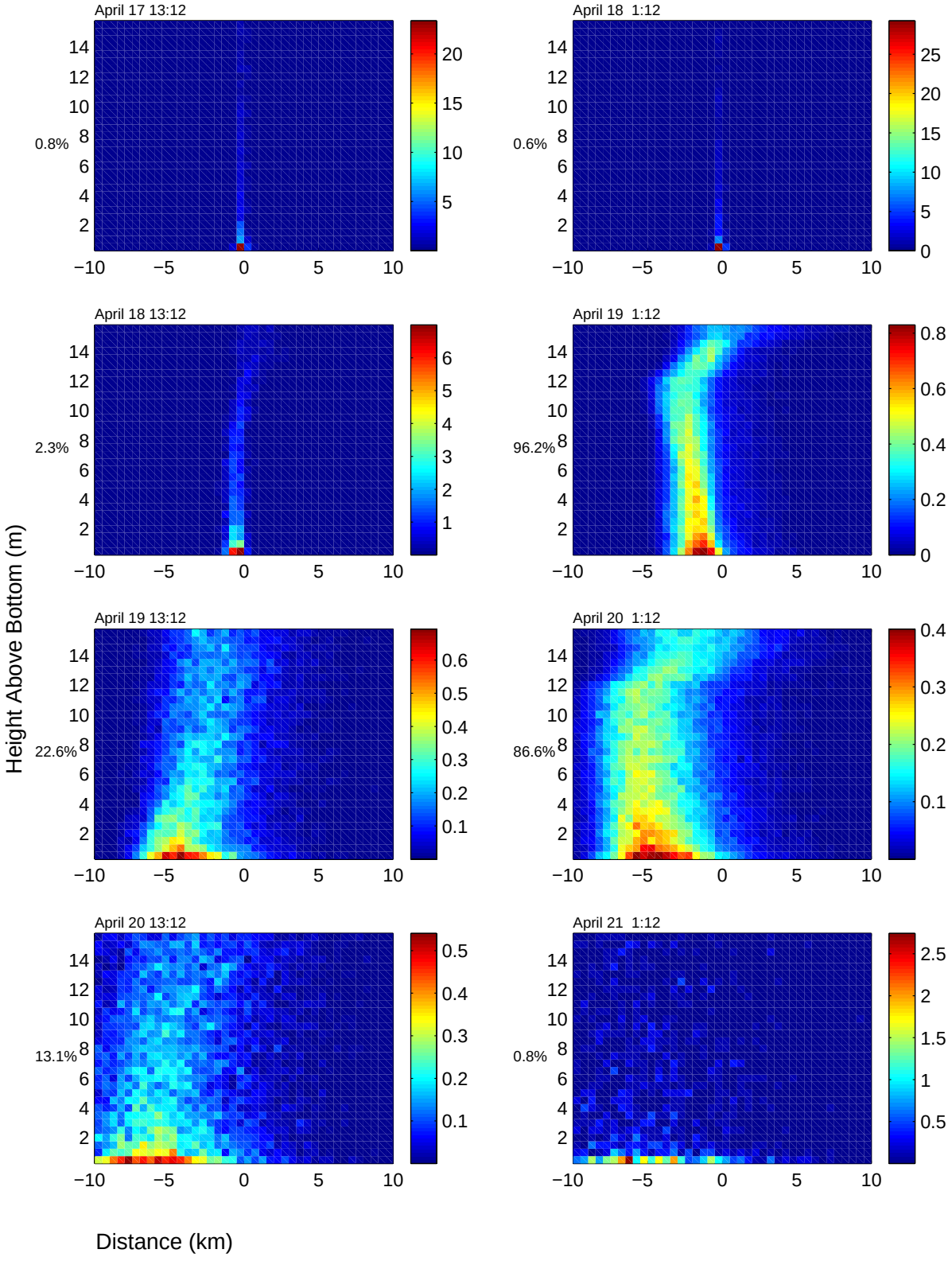

Figure 26. The bblt simulated time series of suspended material during the April current event, 1988.

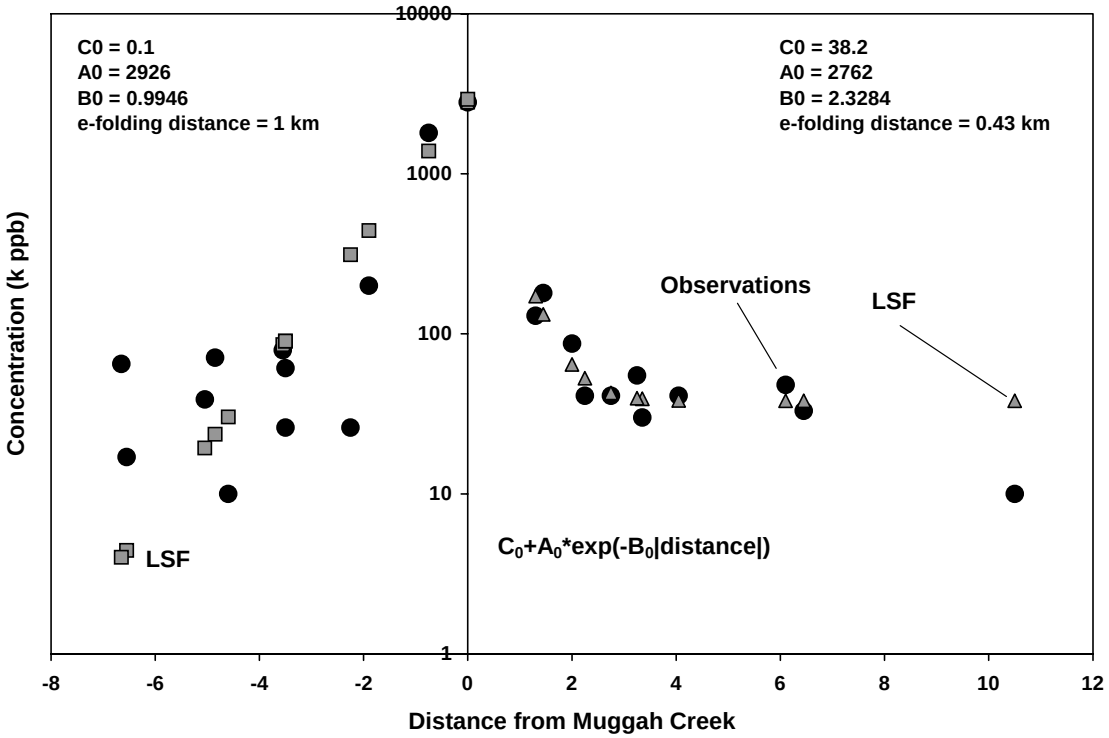

Figure 27. PAH concentrations (in thousands of parts per billion) in bottom sediments from Sydney Harbour (Vandermeulen 1989). Negative (positive) distances are towards the head (mouth). The data have been fitted with a constant plus an exponential (least squares fit).